

Kondo effect in systems with dynamical symmetries

T. Kuzmenko¹, K. Kikoin¹ and Y. Avishai^{1,2}

¹*Department of Physics and ²Ilse Kats Center, Ben-Gurion University, Beer-Sheva, Israel*

(Dated: May 22, 2019)

This paper is devoted to a systematic exposure of the Kondo physics in quantum dots for which the low energy spin excitations consist of a few different spin multiplets $|S_i M_i\rangle$. Under certain conditions (to be explained below) some of the lowest energy levels E_{S_i} are nearly degenerate. The dot in its ground state cannot then be regarded as a simple quantum top in the sense that beside its spin operator other dot (vector) operators \mathbf{R}_n are needed (in order to fully determine its quantum states), which have non-zero matrix elements between states of different multiplets $\langle S_i M_i | \mathbf{R}_n | S_j M_j \rangle \neq 0$. These "Runge-Lenz" operators do not appear in the isolated dot-Hamiltonian (so in some sense they are "hidden"). Yet, they are exposed when tunneling between dot and leads is switched on. The effective spin Hamiltonian which couples the metallic electron spin \mathbf{s} with the operators of the dot then contains new exchange terms, $J_n \mathbf{s} \cdot \mathbf{R}_n$ beside the ubiquitous ones $J_s \mathbf{s} \cdot \mathbf{S}_i$. The operators \mathbf{S}_i and \mathbf{R}_n generate a dynamical group (usually $SO(N)$). Remarkably, the value of N can be controlled by gate voltages, indicating that abstract concepts such as dynamical symmetry groups are experimentally realizable. Moreover, when an external magnetic field is applied then, under favorable circumstances, the exchange interaction involves solely the Runge-Lenz operators \mathbf{R}_n and the corresponding dynamical symmetry group is $SU(N)$. For example, the celebrated group $SU(3)$ is realized in triple quantum dot with four electrons.

PACS numbers: 72.10.-d, 72.15.-v, 73.63.-b

I. INTRODUCTION

Recently, studies of the physical properties of artificially fabricated nano-objects turn out to be a rapidly developing branch of fundamental and applied physics. Progress in these fields is stimulated both by the achievements of nanotechnology and by the ambitious projects of information processing, data storage, molecular electronics and spintronics. The corresponding technological evolution enabled the fabrication of various low-dimensional systems from semiconductor heterostructures to quantum wires and constrictions, quantum dots (QD), molecular bridges and artificial structures with large molecules built in electric circuits¹. This impressive experimental progress led to the development of nanophysics, a new aspect and research direction in quantum physics². Artificial nano-objects possess the familiar features of quantum mechanical systems, but sometimes one may create in artificially fabricated systems such conditions, which are hardly observable "in natura". For example, $1D \rightarrow 2D$ crossover may be realized in quantum networks³ and constrictions⁴. The Kondo effect may be observed in non-equilibrium conditions⁵, at high magnetic fields⁶, and at finite frequencies⁸. Moreover, a quantum dot in the Kondo regime can be integrated into a circuit exhibiting the Aharonov-Bohm effect⁹.

In this paper we focus on an intriguing challenge in this context related to the specific symmetry of the nano-objects under study. More precisely, one is interested in answering questions pertaining to the nature of the underlying symmetry of the dot Hamiltonian and the algebra of operators appearing in the exchange Hamiltonian. The investigation of this topic is intimately related with the geometric structure and electron occupation of the

quantum dot in its ground state. We refer to a quantum dot composed of a single well and containing an odd number N of electrons as a *simple* quantum dot (SQD). The dot Hamiltonian of a SQD (in the absence of an external magnetic field) is composed of two degenerate levels and has an $SU(2)$ symmetry. In that sense the symmetry is referred to as geometrical. The exchange Hamiltonian is expressed in terms of the generators of the group $SU(2)$. On the other hand, quantum dots containing a single well with even N or quantum dots containing several wells are referred to as *composite* quantum dots (CQD). The low energy states of an isolated CQD Hamiltonian are spin multiplets. In the generic case, the only degeneracy is that of magnetic quantum numbers. Yet, as we argue below, dot-lead tunneling results in level renormalization and the emergence of an additional symmetry. To be more precise, we note that 1) The exchange part of the Hamiltonian includes the generators of a non-compact Lie group (usually $SO(n)$ or $SU(n)$) and 2) The *renormalized* low-energy spin-excitation levels of the CQD Hamiltonian are almost degenerate (within a Kondo energy scale). These two aspects are gathered under the term *dynamical symmetry*. A more quantitative exposition will be presented below.

Experimentally, resonance Kondo tunneling was observed in QD with odd electron occupation number under strong Coulomb blockade¹⁰, and in individual atoms and molecules deposited on metallic surfaces and on the edges of metallic wires in break-junction geometry¹¹. According to the theory of Kondo effect in QD¹², the spin degrees of QD are involved in Kondo resonance. In our notation these are SQD and the physics of Kondo tunneling in this case is similar to that of Kondo scattering in magnetically doped metals, at least in the regime of linear response.

The Kondo physics seems to be richer in systems involving tunneling through CQD. Our main purpose is to demonstrate that CQD possesses dynamical symmetries whose realization in Kondo tunneling is experimentally tangible. Such experimental tuning of dynamical symmetries is not possible in conventional Kondo scattering. In many cases even the very existence of Kondo tunneling crucially depends on the dynamical spin symmetry of CQD. Several models dealing with Kondo tunneling in CQDs possessing dynamical symmetry were considered in our previous publications. The case of $SO(4)$ symmetry in double quantum dot (DQD) was studied in Refs. 13,14. A more complicated case of $SO(n)$ symmetry with variable n in a triple quantum dot (TQD) (composed of three potential valleys with intra-well interaction and inter-well tunneling) in parallel geometry is firstly introduced in Ref. 15.

In this paper we develop the general approach to the problem of dynamical symmetries in Kondo tunneling through complex quantum dots and illustrate it by numerous examples of TQD in various configurations, both in parallel and in series geometries. It is shown that our earlier results¹⁵ fall within an elegant pattern of classification of dynamical symmetry groups. The main lesson to be learned is that Kondo physics in CQD suggests a novel and in some sense rather appealing aspect of low-dimensional physics of interacting electrons. It substantiates, in a systematic way, that dynamical symmetry groups play an important role in mesoscopic physics. In particular, we encounter here some "famous" groups which appear in other branches of physics. Thus, the celebrated group $SU(3)$ enters also here when a TQD is subject to an external magnetic field. And the group $SO(5)$ which plays a role in the theory of superconductivity is found here when a certain tuning of the gate voltages in TQD is exercised.

The basic concepts are introduced in section II. First, in sub-section II A, the necessary mathematical ingredients are introduced, although we try to avoid much rigor. Then, in sub-section II B we explain how these abstract concepts can be realized in CQD. In section III the special case of TQD in the parallel geometry is discussed at some length. In sub-section III A we concentrate on the case of even occupation, extending and elaborating upon a short and concise exposition earlier¹⁵. The dynamical-symmetry phase diagram is displayed and the experimental consequences are drawn. The case of odd occupation is exposed in sub-section III B. In section IV a novel phenomena is discussed, namely, *a Kondo effect without a localized spin*. The anisotropic exchange interaction occurs between the metal electron spin and the dot Runge-Lenz operator alone. Finally, in section V we discuss the physics of TQD in a *series* geometry and stress the main difference with the results pertaining to the *parallel* geometry. In the conclusions we underscore the main results obtained here.

The derivation of the pertinent effective spin Hamiltonians and the establishment of group properties (in particu-

lar identification of the group generators and checking the corresponding commutation relations) sometimes require lengthy mathematical expressions. These are collected in the appendices.

II. DYNAMICAL SYMMETRY OF COMPLEX QUANTUM DOTS

A. Generalities

In this section we present in some details the concept of dynamical symmetry, and more particularly, its emergence in CQD. The term *Dynamical Symmetry* implies the symmetry of eigenvectors of a quantum system forming an irreducible representations of a certain Lie group. The main ideas and the relevant mathematical tools can be found, e.g., in Refs. 16. Here we formulate them in a form convenient for our specific purposes without much mathematical rigor. We have in mind a quantum system with Hamiltonian H whose eigenstates $|\Lambda\rangle = |M\mu\rangle$ form (for a given M) a basis to an irreducible representation of some Lie group G . The energies E_M do not depend on the "magnetic" quantum number μ . For definiteness one may think of M as an angular momentum and of μ as its projection, so that G is just $SU(2)$. Now let us look for operators which induce transitions between different eigenstates. An economic way for identifying them is through the Hubbard operators¹⁷

$$X^{\Lambda\Lambda'} = |\Lambda\rangle\langle\Lambda'|. \quad (1)$$

It is natural to divide this set of operators into two subsets. The first one contains the operators $|M\mu\rangle\langle\mu'M|$ while the second one includes operators $|M\mu\rangle\langle\mu'M'|$ for which $|M\mu\rangle$ and $|M'\mu'\rangle$ belong to a *different* representation space of G . A central question at this stage is whether these operators (or rather, certain linear combinations of them) form a close algebra. In some particular cases it is possible to form linear combinations within each set and obtain two new sets of operators $\{S\}$ and $\{R\}$ with the following properties: 1) For a given M the operators $\{S\}$ generate the M irreducible representation of G and commute with H . 2) For a given set M_i the operators $\{S\}$ and $\{R\}$ form an algebra (the *dynamic* algebra) and generate a non-compact Lie group A . The reason for the adjective *dynamic* is that, originally, the operators $\{R\}$ do not appear in the bare Hamiltonian H and emerge only when additional interaction (e.g., dot-dot tunneling) is present. In the special case $G = SU(2)$ the operators in $\{S\}$ are the vector \mathbf{S} of spin operators determining the corresponding irreducible representations, while the operators in the set $\{R\}$ can be grouped into a sequence \mathbf{R}_n of vector operators describing transitions between states belonging to different representations of the $SU(2)$ group.

Strictly speaking, the group A is not a symmetry group of the Hamiltonian H since the operators $\{R\}$ do not

commute with H . Indeed, let us express H in terms of diagonal Hubbard operators,

$$H = \sum_{\Lambda=M\mu} E_\Lambda |\Lambda\rangle\langle\Lambda| = \sum_{\Lambda} E_M X^{\Lambda\Lambda}, \quad (2)$$

so that

$$[X^{\Lambda\Lambda'}, H] = -(E_M - E_{M'}) X^{\Lambda\Lambda'}. \quad (3)$$

As we have mentioned above, the symmetry group of the Hamiltonian H , G , is generated by the operators $X^{\Lambda=M\mu, \Lambda'=M\mu'}$. Remarkably, however, the dynamics of CQD in contact with metallic leads and/or an external magnetic field leads to renormalization of the energies $\{E_M\}$ in such a way that a few levels at the bottom of the spectrum become degenerate, $E_{M_1} = E_{M_2} = \dots = E_{M_n}$. Hence, in this low energy subspace, the group A generated by the operators $\{S\}$ and $\{R\}$ is a symmetry group of H referred to as the dynamical symmetry group. The symbol R is due to the analogy with the Runge-Lenz operator, the hallmark of dynamical symmetry of the Kepler and Coulomb problems¹⁸. Below we will use the term dynamical symmetry also in cases where the levels are not strictly degenerate, their difference is bounded by a certain energy scale, which is the Kondo energy in our special case. In that sense, the symmetry is of course not exact, but rather approximate.

Using the notions of dynamical symmetry, numerous familiar quantum objects, such as hydrogen atom, quantum oscillator in d -dimensions, quantum rotator, may be described in compact and elegant way. We are interested in a special application of this theory, when the symmetry of the quantum system is approximate and its violation may be treated as a perturbation. This aspect of dynamical symmetry was first introduced in particle physics¹⁹, where the classification of hadron eigenstates is given in terms of non-compact Lie groups. In our case, the rotationally invariant object is an isolated quantum dot, whose spin symmetry is violated by electron tunneling to and from the leads under the condition of strong Coulomb blockade.

B. Realization in CQD

The special cases $G = SU(2)$ and $A = SO(n)$ or $SU(n)$ is realizable in CQD. Let us first recall the manner in which the spin vectors appear in the effective low energy Hamiltonian of QD in tunneling contact with metallic leads. When strong Coulomb blockade completely suppresses charge fluctuations in QD, only spin degrees of freedom are involved in tunneling via the Kondo mechanism¹². An *isolated* SQD in this regime is represented solely by its spin vector \mathbf{S} . This is a manifestation of rotational symmetry which is of geometrical origin. The exchange interaction $J\mathbf{s}\cdot\mathbf{S}$ (\mathbf{s} is the spin operator of the metallic electrons) induces transitions between states belonging to the same spin (and breaks $SU(2)$ invariance). On the other hand, the low energy spectrum

of spin excitations in CQD is not characterized solely by its spin operator since there are states close in energy, which belong to different representation spaces of $SU(2)$. Incidentally, these might have either the same spin \mathbf{S} (like, *e.g.*, in two different doublets) or a different spin (like, *e.g.*, in the case of singlet-triplet transitions). The exchange interaction must then contain also other operators \mathbf{R}_n (the R-operators mentioned in the previous sections) inducing transitions between states belonging to different representations. The interesting physics occurs when the operators \mathbf{R}_n “approximately” commute with the Hamiltonian H_{dot} of the isolated dot. In accordance with our previous discussion, the R-operators are expressible in terms of Hubbard operators and have only non-diagonal matrix elements in the basis of the eigenstates of H_{dot} . The spin algebra is then a subalgebra of a more general non-compact Lie algebra formed by the whole set of vectors $\{\mathbf{S}, \mathbf{R}_n\}$. This algebra is characterized by the commutation relations,

$$[S_i, S_j] = it_{ijk} S_k, \quad [S_i, R_{nj}] = it_{ijk} R_{nk}, \\ [R_{ni}, R_{nj}] = it_{ijk}^n S_k, \quad (4)$$

with structure constants t_{ijk} (here ijk are Cartesian indices). The R-operators are orthogonal to \mathbf{S} ,

$$\mathbf{S} \cdot \mathbf{R}_n = 0. \quad (5)$$

In the general case, CQDs possess also other symmetry elements (permutations, reflections, finite rotations). Then, additional scalar generators A_p arise. These generators also may be expressed via original Hubbard operators, and their commutation relations with R-operators have the form

$$[R_{ni}, R_{mj}] = ig_{ij}^{nmp} A_p, \quad [R_{ni}, A_p] = if_{ij}^{nmp} R_{mj}, \quad (6)$$

with structure constants g_{ij}^{nmp} and f_{ij}^{nmp} ($n \neq m$). The operators obeying the commutation relations (4) and (6) form an o_n algebra. The Casimir operator for this algebra is

$$\mathcal{K} = \mathbf{S}^2 + \sum_n \mathbf{R}_n^2 + \sum_p A_p^2. \quad (7)$$

Various representations of all these operators via basic Hubbard operators will be established in the following sections, where the properties of specific CQDs are studied.

Next, we show how the dynamical symmetry of CQD is revealed in the effective spin Hamiltonian describing Kondo tunneling. This Hamiltonian is derived from the generalized Anderson Hamiltonian

$$H_A = H_{dot} + H_{lead} + H_{tun}. \quad (8)$$

The three terms on the right hand side are the dot, lead and tunneling Hamiltonians, respectively. In the generic case, a planar CQD is a confined region of a semiconductor, with complicated multivalley structure secluded

between drain and source leads. The CQD contains several valleys numbered by index a . Some of these valleys are connected with each other by tunnel channels characterized by coupling constants $W_{aa'}$, and some of them are connected with the leads by tunneling. The corresponding tunneling matrix elements are $V_{\alpha a}$ ($\alpha = s, d$ stands for source and drain, respectively). The total number of electrons N in a *neutral* CQD as well as the partial occupation numbers N_a for the separate wells are regulated by Coulomb blockade and gate voltages V_{ga} applied to these wells, with $N = \sum_a N_a$. It is assumed that the capacitive energy for the whole CQD is strong enough to suppress charged states with $N' = N \pm 1$, which may arise in a process of lead-dot tunneling.

If the inter-well tunnel matrix elements $W_{aa'}$ are larger than the dot-lead ones $V_{\alpha a}$ (or if all tunneling strengths are comparable), it is convenient first to diagonalize H_{dot} and then consider H_{tun} as a perturbation. In this case H_{dot} may be represented as

$$H_{dot} = \sum_{\Lambda \in N} E_{\Lambda} |\Lambda\rangle\langle\Lambda| + \sum_{\lambda \in N \pm 1} E_{\lambda} |\lambda\rangle\langle\lambda|. \quad (9)$$

Here all intradot interactions are taken into account. The kets $|\Lambda\rangle \equiv |N, q\rangle$ represent eigenstates of H_{dot} in the charge sector N and quantum numbers q , whereas the kets $|\lambda\rangle \equiv |N \pm 1, p\rangle$ are eigenstates in the charge sectors $N \pm 1$ with quantum numbers p . All other charge states are suppressed by Coulomb blockade. Usually, q and p refer to spin quantum numbers but sometimes other specifications are required (see below).

The lead Hamiltonian takes a simple form

$$H_{lead} = \sum_{k, \alpha, \sigma} \varepsilon_{k\alpha} c_{k\alpha\sigma}^{\dagger} c_{k\alpha\sigma}. \quad (10)$$

This Hamiltonian describes only the simplest situation, when each lead is connected with CQD only by a single tunnel channel, so that the electrons in the lead α are characterized by the wave vector and spin projection k, σ .

The tunnel Hamiltonian involves electron transfer between the leads and the CQD, and thus couples states $|\Lambda\rangle$ of the dot with occupation N and states $|\lambda\rangle$ of the dot with occupation $N \pm 1$. This is best encoded in terms of non-diagonal dot Hubbard operators, which intermix the states from different *charge sectors*

$$X^{\Lambda\lambda} = |\Lambda\rangle\langle\lambda|, \quad X^{\lambda\Lambda} = |\lambda\rangle\langle\Lambda|. \quad (11)$$

Thus,

$$\begin{aligned} H_t = & \sum_{k\alpha a\sigma} \sum_{\lambda \in N+1, \Lambda \in N} \left(V_{\alpha a\sigma}^{\Lambda\lambda} c_{k\alpha\sigma}^{\dagger} |\Lambda\rangle\langle\lambda| + H.c. \right) \\ & + \sum_{k\alpha a\sigma} \sum_{\lambda \in N-1, \Lambda \in N} \left(V_{\alpha a\sigma}^{\lambda\Lambda} c_{k\alpha\sigma}^{\dagger} |\lambda\rangle\langle\Lambda| + H.c. \right) \end{aligned} \quad (12)$$

where $V_{\alpha a\sigma}^{\lambda\Lambda} = V_{\alpha a} \langle \lambda | d_{a\sigma} | \Lambda \rangle$.

Before turning to calculation of CQD conductance, the relevant energy scales should be specified. First, we

suppose that the bandwidth of the continuum states in the leads, D_{α} , substantially exceeds the tunnel coupling constants, $D_{\alpha} \gg W_{aa'}$, $V_{\alpha a}$ (actually, we consider leads made of the same material with $D_l = D_r = D_0$.) Second, each well a in the CQD is characterized by the "activation energy" defined as $\Delta_a = E_{\Lambda}(N_a) - E_{\lambda}(N_a - 1)$, i.e., the energy necessary to extract one electron from the well containing N_a electrons and move it to the Fermi level of the leads (the Fermi energy is used as the reference zero energy level from now on). Note that Δ_a is tunable by applying the corresponding gate voltage V_{ga} . We are mainly interested in situations where the condition

$$\Delta_c \sim D_a, \quad Q_c, \quad (13)$$

is satisfied at least for one well labeled by the index c . Here Q_c is a capacitive energy, which is predetermined by the radius of the well c . Eventually, this well with the largest charging energy is responsible for Kondo-like effects in tunneling, provided the occupation number N_c is odd. The third condition assumed in our model is a weak enough Coulomb blockade in all other wells except that with $a = c$, i.e., $Q_a \ll Q_c$. Finally, we demand that

$$b_{\alpha a} \equiv \frac{V_{\alpha a}}{\Delta_a} \ll 1, \quad (14)$$

for those wells, which are coupled with metallic leads, and

$$\beta_a = \frac{W_{ac}}{E_{ac}} \ll 1. \quad (15)$$

Here E_{ac} are the charge transfer energies for electron tunneling from the c -well to other wells in the CQD.

The interdot coupling under Coulomb blockade in each well generates indirect exchange interactions between electrons occupying different wells. Diagonalizing the dot Hamiltonian for a *given* $N = \sum_a N_a$, one easily finds that the low-lying spin spectrum in the charge sectors with even occupation N consists of singlet/triplet pairs (spin $S = 0$ or 1, respectively). In charge sectors with odd N the manifold of spin states consists of doublets and quartets (spin $S=1/2$ and $3/2$, respectively).

The resonance Kondo tunneling is observed as a temperature dependent zero bias anomaly in tunnel conductance¹⁰. According to existing theoretical understanding, the quasielastic cotunneling accompanied by the spin flip transitions in a quantum dot is responsible for this anomaly. To describe the cotunneling through a neutral CQD with given N , one should integrate out transitions involving high-energy states from charge sectors with $N' = N \pm 1$. In the weak coupling regime at $T > T_K$ this procedure is done by means of perturbation theory which can be employed in a compact form within the renormalization group (RG) approach formulated in Refs. 20,21.

As a result of the RG iteration procedure, the energy levels E_{Λ} in the Hamiltonian (9) are renormalized and

indirect exchange interactions between the CQD and the leads arise. The RG procedure is equivalent to summation of the perturbation series at $T > T_K$, where T_K is the Kondo energy characterizing the crossover from a perturbative weak coupling limit to a non-perturbative strong coupling regime. The leading logarithmic approximation of perturbation theory corresponds to a single-loop approximation of RG theory. In this approximation the tunnel constants W and V are not renormalized, as well as the charge transfer energy Δ_c (13). Reduction of the energy scale from the initial value D_0 to a lower scale $\sim T$ results in renormalization of the energy levels $E_\Lambda \rightarrow \bar{E}_\Lambda(D_0/T)$ and a generation of an indirect exchange interaction between the dot and the leads with an (antiferromagnetic) exchange constant J .

The rotational symmetry of a *simple* quantum dot is broken by the spin-dependent interaction with the leads, which arises in second order in the tunneling amplitude V_α . In complete analogy, the *dynamical symmetry* of a *composite* quantum dot is exposed (broken) as encoded in the effective exchange Hamiltonian. In a generic case, there are, in fact, several exchange constants arranged within an exchange matrix J which is non-diagonal both in dot and lead quantum numbers. The corresponding exchange Hamiltonian is responsible for spin-flip assisted cotunneling through the CQD as well as for singlet-triplet transitions.

The precise manner in which these statements are quantified will now be explained. After completing the RG procedure, one arrives at an effective (or renormalized) Hamiltonian \bar{H} in a reduced energy scale \bar{D} ,

$$\bar{H} = \bar{H}_{dot} + \bar{H}_{lead} + \bar{H}_{cotun}, \quad (16)$$

where the effective dot Hamiltonian (9) is reduced to

$$\bar{H}_{dot} = \sum_{\Lambda \in N} \bar{E}_\Lambda X^{\Lambda\Lambda} \quad (17)$$

written in terms of *diagonal* Hubbard operators,

$$X^{\Lambda\Lambda} = |\Lambda\rangle\langle\Lambda|. \quad (18)$$

At this stage, the manifold $\{\Lambda\} \in N$ contains only the renormalized low-energy states within the energy interval comparable with T_K (to be defined below). Some of these states may be quasi degenerate, with energy differences $|\bar{E}_\Lambda - \bar{E}_{\Lambda'}| < T_K$. However, T_K itself is a function of these energy distances (see, e.g.,^{6,22,23}), and all the levels, which influence T_K , should be retained in (17).

The effective cotunneling Hamiltonian acquires the form

$$H_{cot} = \sum_{\alpha\alpha'} \left(J_0^{\alpha\alpha'} \mathbf{S} \cdot \mathbf{s}^{\alpha\alpha'} + \sum_n J_n^{\alpha\alpha'} \mathbf{R}_n \cdot \mathbf{s}^{\alpha\alpha'} \right). \quad (19)$$

Here \mathbf{S} is the spin of CQD in its ground state, the operators $\mathbf{s}^{\alpha\alpha'}$ represent the spin states of lead electrons,

$$\mathbf{s}^{\alpha\alpha'} = \frac{1}{2} \sum_{kk'} \sum_{\sigma\sigma'} c_{k\alpha\sigma}^\dagger \hat{\tau}_{\sigma\sigma'} c_{k'\alpha'\sigma'}, \quad (20)$$

where $\hat{\tau}$ is the vector of Pauli matrices. In the conventional Kondo effect the logarithmic divergent processes develop due to spin reversals given by the first term containing the operator \mathbf{S} . In CQD possessing dynamical symmetry, all R-vectors are involved in Kondo tunneling. In the following sections we will show how these additional processes are manifested in resonance Kondo tunneling through CQD. Note that the elements of the matrix J are also subject to temperature dependent renormalization $J_n^{\alpha\alpha'} \rightarrow J_n^{\alpha\alpha'}(D_0/T)$.

The cotunneling Hamiltonian (19) is the natural generalization of the conventional Kondo Hamiltonian $J\mathbf{s}\cdot\mathbf{S}$ for CQDs possessing dynamical symmetries. In many cases there are several dot spin 1 operators depending on which pair of electrons is “active”. In this pair, one electron sits in well c and the other one sits in some well a . The other $N - 2$ electrons are paired in singlet states (recall that N is even). The spin 1 operator for the active pair is denoted as \mathbf{S}_a . (In some sense, the need to specify which pair couples to $S = 1$ while all other pairs are coupled to $S = 0$ is the analog of the seniority scheme in atomic and nuclear physics (see, e.g.,⁷)). The cotunneling Hamiltonian for CQD contains exchange terms $J_0^{\alpha\alpha'} \mathbf{S}_a \cdot \mathbf{s}^{\alpha\alpha'}$. Then, instead of a single exchange term (first term on the RHS in Eq. (19)), one has a sum $\sum_a J_a^{\alpha\alpha'} \mathbf{S}_a \cdot \mathbf{s}^{\alpha\alpha'}$. Additional symmetry elements (finite rotations and reflections) turn the cotunneling Hamiltonian even more complicated. In the following sections we will consider several examples of such CQDs. It is seen from (19), that in the generic case, both spin and R-vectors may be the sources of anomalous Kondo resonances. The contribution of these vectors depends on the hierarchy of the energy states in the manifold. In principle, it may happen that the main contribution to the Kondo tunneling is given not by the spin of the dot, but by one of the R-vectors.

Thus, we arrive at the conclusion that the regular procedure of reducing the full Hamiltonian of a quantum dot in junctions with metallic leads to an effective Hamiltonian describing only spin degrees of freedom of this system reveals a rich dynamical symmetry of CQD. Strictly speaking, only an isolated QD with $N = 1$ is fully described by its spin 1/2 obeying $SU(2)$ symmetry without dynamical degrees of freedom. Yet the doubly occupied dot with $N = 2$ possesses the dynamical symmetry of a *spin rotator* because its spin spectrum consists of a singlet ground state (S) and a triplet excitation (T). Therefore, an R-vector describing S/T transitions may be introduced, and the Kondo tunneling through a dot of this kind may involve spin excitation under definite physical conditions, e.g., in an external magnetic field⁶. A two-electron quantum dot under Coulomb blockade constitutes apparently the simplest non-trivial example of a nano-object with dynamical symmetry of a spin rotator possessing an $SO(4)$ symmetry.

Dynamical symmetries $SO(n)$ of CQDs are described by non-compact semi-simple algebras²⁴. This non-compactness implies that the corresponding algebra o_n

may be presented as a direct sum of subalgebras, e.g., $o_4 = o_3 \oplus o_3$. Therefore, the dynamical symmetry group may be presented as a direct product of two groups of lower rank. In case of spin rotator the product is $SO(4) = SU(2) \otimes SU(2)$. Generators of these subgroups may be constructed from those of the original group. The $SO(4)$ group possesses a single R-operator \mathbf{R} , and the direct product is realized by means of the transformation

$$\mathbf{K} = \frac{\mathbf{S} + \mathbf{R}}{2}, \quad \mathbf{N} = \frac{\mathbf{S} - \mathbf{R}}{2}. \quad (21)$$

Both vectors \mathbf{K} and \mathbf{N} generate $SU(2)$ symmetry and may be treated as fictitious $S=1/2$ spins²². In some situations these vectors are real spins localized in different valleys of CQD. In particular, the transformation (21) maps a single site Kondo problem for a DQD possessing $SO(4)$ symmetry to a two-site Kondo problem for spin 1/2 centers with an $SU(2)$ symmetry (see discussion in Refs. 13,14). For groups of higher dimensionality ($n \geq 4$) one can use many different ways of factorization, which may be represented by means of different Young tableaux (see Appendix D).

Even in the case $n = 4$, the transformation (21) is not the only possible "two-spin" representation. An alternative representation is realized in an external magnetic field¹⁴. When the ground state of S/T manifold is singlet (the energy $\delta = E_T - E_S > 0$), the Zeeman splitting energy of a triplet in an external magnetic field may exactly compensate the exchange splitting δ . This occasional degeneracy is described by the pseudospin 1/2 formed by the singlet and the up projection of spin 1 triplet. Two other projections of the triplet form the second pseudospin 1/2. The Kondo effect induced by external magnetic field observed in several nano-objects²⁵, was the first experimental manifestation of dynamical symmetry in quantum dots.

We outlined in this section the novel features which appear in effective Kondo Hamiltonians due to the dynamical symmetry of CQD exhibiting Kondo tunneling. In the following sections we will see how the additional terms in the Hamiltonian (19) influence the properties of Kondo resonance in various structures of CQDs.

III. TRIPLE QUANTUM DOT IN PARALLEL GEOMETRY

So far we briefly mentioned the simplest structure of CQD, i.e., double quantum dot with occupation $N = 2$ and employed it to describe some generic properties of CQD enumerated in the previous section. This kind of an artificial molecule is the analog of a hydrogen molecule in the Heitler-London limit^{13,14}, and its $SO(4)$ symmetry reflects the spin properties of ortho/parahydrogen. A much richer artificial object is a triple quantum dot (TQD), which can be considered as an analog of a *linear molecule* RH_2 . The central (c) dot is assumed to have a

smaller radius (and, hence, larger capacitive energy Q_c) than the left (l) and right (r) dots, i.e., $Q_c \gg Q_{l,r}$. Fig. 1 illustrates this configuration in a parallel geometry, where the "left-right" ($l-r$) reflection plane of the TQD is perpendicular to the "source-drain" ($s-d$) reflection plane of metallic electrodes.

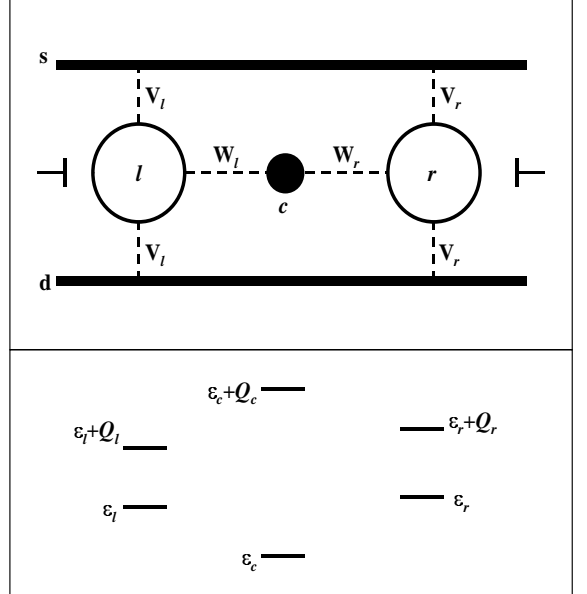


FIG. 1: Triple quantum dot in parallel geometry and energy levels of each dot $\varepsilon_a = \varepsilon_a - V_{ga}$ (bare energy minus gate voltage).

To regulate the occupation of TQD as a whole and its constituents in particular, there are a couple of gates V_{gl}, V_{gr} applied to the l, r dots. The energy levels of single- and two-electron states in each one of the three constituent dots are shown in the lower panel of Fig. 1. Here the gate voltages $V_{gl,r}$ are applied in such a way that the one-electron level ε_c of a c -dot is essentially deeper than those of the l, r -dots, so that the condition (13) is satisfied for the c dot, whereas the inequalities (14) and (15) are satisfied for the "active" l and r dots. Tunneling between the side dots l, r and the central one c with amplitudes $W_{l,r}$ determines the low energy spin spectrum of the isolated TQD once its occupation N is given. This system possesses much richer dynamical properties than the DQD mentioned above, first of all, because it allows the study of dynamical symmetry both for even and odd occupation N . To reveal the difference between oddly and evenly occupied dots it is sufficient to consider two cases, namely $N = 4$ and $N = 3$. The former case was briefly analyzed in Ref. 15. Here we study the Kondo tunneling through TQD in more details and in both configurations.

The full diagonalization procedure of the Hamiltonian H_{dot} for the TQD is presented in Appendix A. When the condition (15) is valid, the low-energy manifold for $N = 4$ is composed of two singlets $|S_l\rangle, |S_r\rangle$, two triplets $|T_a\rangle = |\mu_a\rangle$ ($a = l, r, \mu_a = 1_a, 0_a, \bar{1}_a$) and a charge trans-

fer singlet exciton $|Ex\rangle$ with an electron removed from the c -well to the "outer" wells. The corresponding energies are,

$$\begin{aligned} E_{S_a} &= \epsilon_c + \epsilon_a + 2\epsilon_{\bar{a}} + Q_{\bar{a}} - 2W_a\beta_a, \\ E_{T_a} &= \epsilon_c + \epsilon_a + 2\epsilon_{\bar{a}} + Q_{\bar{a}}, \\ E_{Ex} &= 2\epsilon_l + 2\epsilon_r + Q_l + Q_r + 2W_l\beta_l + 2W_r\beta_r, \end{aligned} \quad (22)$$

where the charge transfer energies in Eq. (15) for determining β_a are $E_{ac} = Q_a + \epsilon_a - \epsilon_c$; the notation $a = l, r$ and $\bar{a} = r, l$ is used ubiquitously hereafter.

For odd occupation $N = 3$, the low-energy spin multiplet contains two spin 1/2 doublets $|D_{1,2}\rangle$ and a spin quartet $|Q\rangle$,

$$\begin{aligned} E_{D_1} &= \epsilon_c + \epsilon_l + \epsilon_r - \frac{3}{2} [W_l\beta_l + W_r\beta_r], \\ E_{D_2} &= \epsilon_c + \epsilon_l + \epsilon_r - \frac{1}{2} [W_l\beta_l + W_r\beta_r], \\ E_Q &= \epsilon_c + \epsilon_l + \epsilon_r. \end{aligned} \quad (23)$$

There are also four charge-transfer excitonic counterparts of the spin doublets separated by the charge transfer gaps $\sim \epsilon_l - \epsilon_c + Q_l$ and $\epsilon_r - \epsilon_c + Q_r$ from the above states (see Appendix A). Consideration of these two examples provide us with an opportunity to investigate the dynamical symmetry of CQD with integer and half-integer spin.

A. Even occupation

We commence with the case of TQD with even occupation $N = 4$ briefly discussed in Ref. 15. This configuration is a direct generalization of an asymmetric spin rotator, i.e., the double quantum dot in a side-bound geometry¹³. Compared with the asymmetric DQD, this composite dot possesses one more symmetry element, i.e., the $l - r$ permutation, which, as will be seen below, enriches the dynamical properties of CQD.

Following a glance at the energy level scheme (22), one is tempted to conclude outright that for finite W , the ground state of this TQD configuration is a singlet and consequently there is no room for the Kondo effect to take place. A more attentive study of the tunneling problem, however, shows that *tunneling between the TQD and the leads opens the way for a rich Kondo physics accompanied by numerous dynamical symmetries*.

Indeed, inspecting the expressions for the energy levels, one sees that the singlet states E_{S_a} are modified due to inter-well tunneling, whereas the triplet states E_{T_a} are left intact. This difference is due to the admixture of the singlet states with the charge transfer singlet exciton (see Appendix A). As was mentioned in the previous section, the Kondo cotunneling in the perturbative weak coupling regime at $T, \varepsilon > T_K$ is excellently described within RG formalism^{20,21}. According to general prescriptions of this theory, the renormalizable parameters of the effective low-energy Hamiltonian in a one-loop approximation are

the energy levels E_Λ and the effective indirect exchange vertices $J_{\Lambda\Lambda'}^{\alpha\alpha'}$. Figure 2 illustrates the renormalization

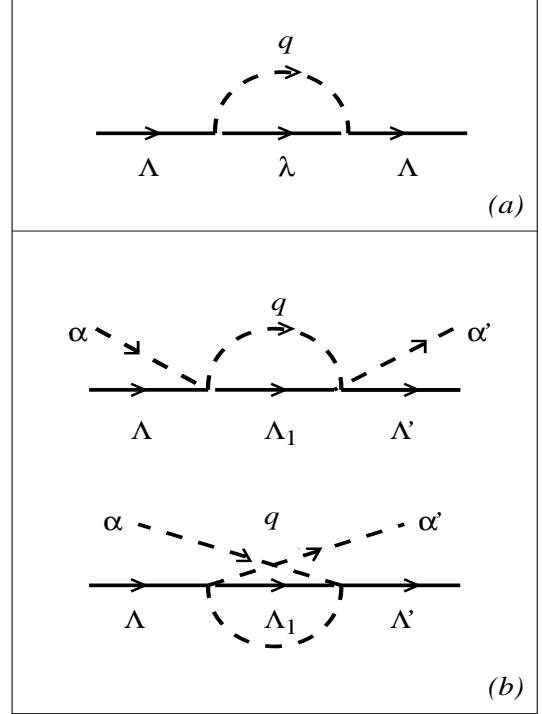


FIG. 2: RG diagrams for the energy levels E_Λ (a) and the effective exchange vertices $J_{\Lambda\Lambda'}^{\alpha\alpha'}$ (b) (see text for further explanations).

processes which contribute to these parameters. The intermediate states in these diagrams are the high-energy states $|q\rangle$ near the ultraviolet cut-off energy D of the band continuum in the leads (dashed lines) and the states $|\lambda\rangle$ from adjacent charge sectors, which are admixed with the low-energy states $|\Lambda\rangle \in N$ by the tunneling Hamiltonian H_t (12) (full lines). Due to the condition (13), the central dot c remains "passive" throughout the RG procedure. The mathematical realization of the diagrams displayed in Fig.2a is encoded in the scaling equations

$$\pi dE_\Lambda/dD = \sum_\lambda \frac{\Gamma_\Lambda}{D - E_{\Lambda\lambda}}. \quad (24)$$

Here $E_{\Lambda\lambda} = E_\Lambda - E_\lambda$, $\Gamma_\Lambda = \pi\rho_0|V^{\Lambda\lambda}|^2$ are the tunnel coupling constants which are different for different Λ ,

$$\Gamma_{T_a} = \pi\rho_0(V_a^2 + 2V_{\bar{a}}^2), \quad \Gamma_{S_a} = \alpha_a^2\Gamma_{T_a}, \quad (25)$$

with $\alpha_a = \sqrt{1 - 2\beta_a^2}$, and ρ_0 is the density of electron states in the leads, which is supposed to be energy independent. These scaling equations should be solved at some initial conditions

$$E_\Lambda(D_0) = E_\Lambda^{(0)}, \quad (26)$$

where index (0) marks the bare values of the model parameters entering the Hamiltonian H_A (8).

Due to the above mentioned dependence of tunneling rates on the index Λ , namely the possibility of $\Gamma_T > \Gamma_S$, the scaling trajectories $E_\Lambda(D)$ may cross at some value of the monotonically decreasing energy parameter D . The nature of level crossing is predetermined by the initial conditions (26) and the ratios between the tunneling rates Γ_Λ . As long as the inequality $|E_{\Lambda\lambda}| \ll D$ is effective, the scaling equations (24) may be approximated as

$$\pi dE_\Lambda/d\ln D = \Gamma_\Lambda. \quad (27)$$

The scaling trajectories are determined by the scaling invariants for equations (24),

$$E_\Lambda^* = E_\Lambda(D) - \pi^{-1}\Gamma_\Lambda \ln(\pi D/\Gamma_\Lambda), \quad (28)$$

tuned to satisfy the initial conditions. With decreasing energy scale D these trajectories flatten and become D -independent in the so called Schrieffer-Wolff (SW) limit, which is reached when the activation energies Δ_a become comparable with D . The corresponding effective bandwidth is denoted as \bar{D} (we suppose, for the sake of simplicity, that $\Delta_a < Q_a$, so that only the states $|\lambda\rangle$ with $N' = N - 1$ are relevant). If this remarkable level crossing occurs at $D > \bar{D}$, we arrive at the situation where *adding an indirect exchange interaction between the TQD and the leads changes the magnetic state of the TQD from singlet to triplet*. Those states E_Λ , which remain close enough to the new ground state are involved in the Kondo tunneling. As a result, the TQD acquires a rich dynamical symmetry structure instead of the trivial symmetry of spin singlet predetermined by the initial energy level scheme (22).

Various cases of non-trivial dynamical symmetry of TQD with $N = 4$ are presented in Figs. 3, 4, 5. It is seen

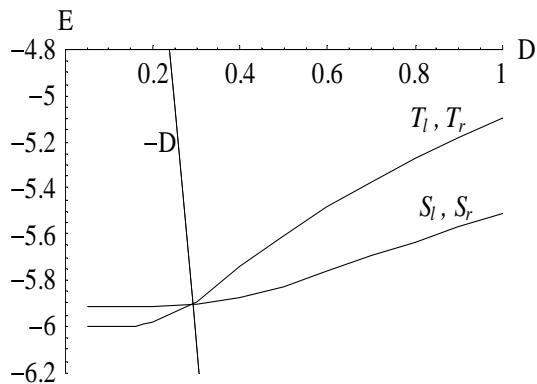


FIG. 3: Scaling trajectories for $P \times SO(4) \times SO(4)$ symmetry in the SW regime.

from these figures that in the most degenerate state, all trajectories reach the SW limit at nearly the same value of D , and the whole octet of spin singlets and triplets forming the manifold (22) is intermixed by the tunnel operator H_t (12). At this stage, the SW procedure for

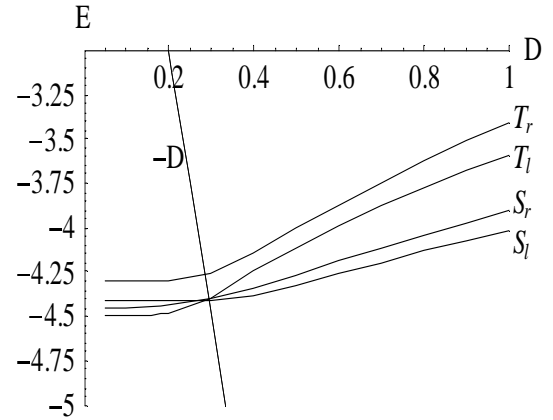


FIG. 4: Scaling trajectories resulting in an $SO(5)$ symmetry in the SW regime.

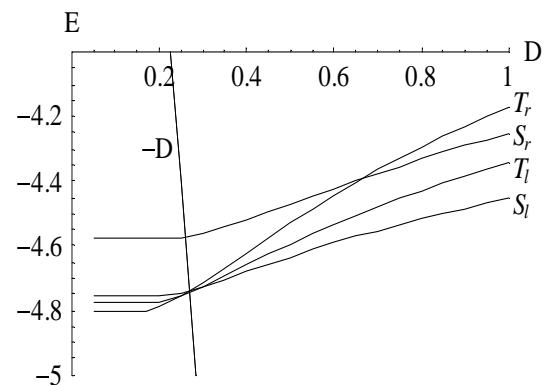


FIG. 5: Scaling trajectories for $SO(7)$ symmetry in the SW regime.

constructing the effective spin Hamiltonian in the subspace $\mathbb{R}_8 = \{T_l, S_l, T_r, S_r\}$ should be applied. This procedure excludes the charged states generated by H_t to second order in perturbation theory (see, e.g.,²⁶).

In parallel geometry one can exclude the non-diagonal tunneling terms $\sim J^{sd}$ by a simple rotation in a $s - d$ space,

$$c_\zeta = \sum_\alpha M_{\zeta\alpha} c_\alpha, \quad (29)$$

where $\zeta = g, u$ stands for the even and odd combination of the lead states $\alpha = s, d$, $M_{\zeta\alpha}$ are the elements of the corresponding rotation matrix M^{12} . As a result of this rotation the odd combinations $\zeta = u$ are decoupled and do not appear in the effective spin Hamiltonian. We are then left with g states only. Having this in mind, we omit the lead index in all cases where the above rotation is operative.

Returning back to the SW transformation, one should note that unlike the case of DQD studied in Refs. 13,14, where the spin operators are the total spin \mathbf{S} and a single R-operator, describing S/T transitions, the TQD is represented by several spin operators corresponding to

different Young tableaux (see Appendix D). The general procedure of deriving the effective spin Hamiltonian is presented in Appendix B. When all the states in the above octet \mathbb{R}_8 are non-degenerate, the effective spin Hamiltonian describing the cotunneling to order $O(|V|^2)$ acquires the form

$$\begin{aligned} H_{\text{cot}} = & \sum_{\Lambda_a} \bar{E}_{\Lambda_a} X^{\Lambda_a \Lambda_a} + \sum_{k\sigma} \varepsilon_k c_{k\sigma}^\dagger c_{k\sigma} \\ & + \sum_{a=l,r} (J_a^T + J_{lr} \hat{P}) \mathbf{S}_a \cdot \mathbf{s} \\ & + \sum_{a=l,r} J_a^{ST} \mathbf{R}_a \cdot \mathbf{s} + \sum_{a=l,r} J_{lr} \tilde{\mathbf{R}}_a \cdot \mathbf{s}. \end{aligned} \quad (30)$$

Here we recall that $\bar{E}_{\Lambda_a} = E_{\Lambda_a}(\bar{D})$, and the effective exchange constants are

$$\begin{aligned} J_a^T &= \frac{2V_a^2}{\epsilon_F - \epsilon_a}, \quad J_a^{ST} = \alpha_a J_a^T, \\ J_{lr} &= V_l V_r \left(\frac{1}{\epsilon_F - \epsilon_l} + \frac{1}{\epsilon_F - \epsilon_r} \right). \end{aligned} \quad (31)$$

The spin operator of conduction electrons is presented by the diagonal term $\mathbf{s} \equiv \mathbf{s}^{gg}$ (cf. (20)). The vector operators $\mathbf{S}_a, \mathbf{R}_a, \tilde{\mathbf{R}}_a$ and the permutation operator \hat{P} manifest the dynamical symmetry of TQD in a subspace \mathbb{R}_8 . The permutation operator

$$\hat{P} = \sum_{a=l,r} \left(X^{S_a S_{\bar{a}}} + \sum_{\mu=1,0,\bar{1}} X^{\mu_a \mu_{\bar{a}}} \right), \quad (32)$$

commutes with $\mathbf{S}_l + \mathbf{S}_r$ and $\mathbf{R}_l + \mathbf{R}_r$.

The spherical components of these vectors are defined via Hubbard operators connecting different states of the octet, $\mathbf{s} = (S_a^+, S_a^-, S_a^z)$, $\mathbf{R} = (R_a^+, R_a^-, R_a^z)$, $\tilde{\mathbf{R}} = (\tilde{R}_a^+, \tilde{R}_a^-, \tilde{R}_a^z)$.

$$\begin{aligned} S_a^+ &= \sqrt{2}(X^{1_a 0_a} + X^{0_a \bar{1}_a}), & S_a^- &= (S_a^+)^{\dagger}, \\ S_a^z &= X^{1_a 1_a} - X^{\bar{1}_a \bar{1}_a}, & & \\ R_a^+ &= \sqrt{2}(X^{1_a S_a} - X^{S_a \bar{1}_a}), & R_a^- &= (R_a^+)^{\dagger}, \\ R_a^z &= -(X^{0_a S_a} + X^{S_a 0_a}), & & \\ \tilde{R}_a^+ &= \sqrt{2}(\alpha_{\bar{a}} X^{1_a S_{\bar{a}}} - \alpha_a X^{S_a \bar{1}_{\bar{a}}}), & \tilde{R}_a^- &= (\tilde{R}_a^+)^{\dagger}, \\ \tilde{R}_a^z &= -(\alpha_{\bar{a}} X^{0_a S_{\bar{a}}} + \alpha_a X^{S_a 0_{\bar{a}}}). & & \end{aligned} \quad (33)$$

Additional symmetry element (l-r permutation) resulted in more complicated algebra which involves the R-operator $\tilde{\mathbf{R}}$ and the scalar operators A intermixing l and r components of TQD.

One can derive from the generic Hamiltonian (30) more symmetric effective Hamiltonians describing partly degenerate configurations illustrated by the flow diagrams of Figs. 3,4,5. We start with the most symmetric case (Fig. 3), where the renormalized spectrum is formed by two triplets $E_{T_l} = E_{T_r} \equiv E_T$ and two singlets $E_{S_l} = E_{S_r} \equiv E_S$. This regime is realized for initial conditions $E_{lc} = E_{rc}$ and $\Gamma_{\Lambda_l} = \Gamma_{\Lambda_r}$ (see Eq. 15). Now

the permutation \hat{P} (32) is the symmetry operation of the Hamiltonian (30). When $\alpha_l = \alpha_r \equiv \alpha$ the equality $\tilde{\mathbf{R}} = \hat{P} \mathbf{R}$ is valid, and the exchange part of the Hamiltonian (30) for symmetric TQD takes the form

$$H_{\text{cot}} = \sum_{a=l,r} (1 + \hat{P})(J^T \mathbf{S}_a + J^{ST} \mathbf{R}_a) \cdot \mathbf{s}. \quad (34)$$

The operator algebra is given by the commutation relations which is a generalization of the o_4 algebra,

$$\begin{aligned} [S_{aj}, S_{a'k}] &= ie_{jkm} \delta_{aa'} S_{am}, \\ [R_{aj}, R_{a'k}] &= ie_{jkm} \delta_{aa'} S_{am}, \\ [R_{aj}, S_{a'k}] &= ie_{jkm} \delta_{aa'} R_{am}. \end{aligned} \quad (35)$$

The operators \mathbf{S}_a are orthogonal to \mathbf{R}_a , and the Casimir operators in this case are $\mathcal{K}_a = \mathbf{S}_a^2 + \mathbf{R}_a^2 = 3$. This justifies the qualification of such TQD as a *double spin rotator* which is obtained from the spin rotator considered in Refs.^{13,14} by a mirror reflection. The symmetry of such TQD is $P \times SO(4) \times SO(4)$.

If $\delta_a = \bar{E}_S - \bar{E}_T \sim T_K$, the dynamical symmetry of the TQD responsible for Kondo tunneling is determined by all these states. We are left here with two coupling constants J^T and J^{ST} , which are renormalized due to Kondo screening. By means of the RG procedure similar to that of Ref.²⁰, the scaling equations are derived,

$$\frac{dj_1}{d \ln d} = -2[(j_1)^2 + (j_2)^2], \quad \frac{dj_2}{d \ln d} = -4j_1 j_2, \quad (36)$$

with $j_1 = \rho_0 J^T, j_2 = \rho_0 J^{ST}, d = \rho_0 D$. In the limit of complete degeneracy the system (36) is reduced to a single equation,

$$\frac{dj_+}{d \ln d} = -2(j_+)^2, \quad (37)$$

for $j_+ = j_1 + j_2$. Its solution yields the Kondo temperature

$$T_{K0} = \bar{D} \exp \left\{ -\frac{1}{2j_+} \right\}, \quad (38)$$

which is an obvious generalization of that derived for a QD with $SO(4)$ symmetry and triplet ground state^{6,13,14}. In the general case T_K is a function of δ , because the scaling of j_2 terminates at $D \approx \delta$ (cf.^{6,22}). Analytic solution of Eqs. (36) may be obtained for large positive δ , so that $\delta \gg T_{K0}$. In this case $j_2 \approx \alpha j_1$ and

$$\frac{T_K}{T_{K0}} \approx \left(\frac{T_{K0}}{\delta} \right)^\alpha. \quad (39)$$

In the asymptotic limit of $\delta \rightarrow \bar{D}$ the singlet state should be excluded from the manifold, together with the last term $\sim J^{ST}$ in the Hamiltonian (34). The symmetry of the TQD with spin one in this case is $P \times SO(3) \times SO(3)$.

It should be emphasized that the Hamiltonian (34) *cannot* be treated as a generalization of a two-site Kondo

Hamiltonian in spite of the fact that the TQD is represented by two spin operators in Kondo screening terms. The reason is that unlike the standard two-site Kondo problem²⁷, the states $|\Lambda\rangle = |S_a\rangle, |T_a\rangle$ for $a = l, r$ are orthogonal because they belong to the same manifold and differ only in symmetrization scheme (see Appendix D for corresponding Young tableaux). As a result, the identities

$$S_a^i S_{\bar{a}}^j = 0, \quad R_a^i R_{\bar{a}}^j = 0$$

are valid (see Eq. 33), and the two-site vertices are not generated by the RG iterations. Thus the Kondo effect for the TQD with mirror symmetry is characterized by the stable infinite fixed point characteristic for the *underscreened* spin one dot, similar to that for DQD^{13,14}. The only manifestation of this symmetry is the additional factor 1/2 in the Kondo exponent T_{K0} (38).

Now we turn to asymmetric configurations where $E_{lc} \neq E_{rc}$, $\Gamma_{Tr} \neq \Gamma_{Tl}$. When $\bar{E}_{Sl} \approx \bar{E}_{Tl} \approx \bar{E}_{Sr} < \bar{E}_{Tr}$ (Fig. 4), the TQD possesses an $SO(5)$ symmetry of a manifold $\{T_l, S_l, S_r\}$. The group generators of the o_5 algebra are the l -vectors $\mathbf{S}_l, \mathbf{R}_l$ from (33) and the operators intermixing l - and r -states, namely the vector $\tilde{\mathbf{R}}$,

$$\begin{aligned} \tilde{R}^+ &= \sqrt{2}(X^{1_l S_r} - X^{S_r \bar{1}_l}), & \tilde{R}^- &= (\tilde{R}^+)^{\dagger}, \\ \tilde{R}^z &= -(X^{0_l S_r} + X^{S_r 0_l}), & & \end{aligned} \quad (40)$$

and scalar A

$$A = i(X^{S_r S_l} - X^{S_l S_r}). \quad (41)$$

The commutation relations (4),(6) in this particular case acquire the form

$$\begin{aligned} [S_{lj}, S_{lk}] &= ie_{jkm} S_{lm}, & [R_{lj}, R_{lk}] &= ie_{jkm} S_{lm}, \\ [\tilde{R}_j, S_{lk}] &= ie_{jkm} \tilde{R}_m, & [\tilde{R}_j, \tilde{R}_k] &= ie_{jkm} S_{lm}, \\ [R_{lj}, S_{lk}] &= ie_{jkm} R_{lm}, & [R_{lj}, \tilde{R}_k] &= i\delta_{jk} A, \\ [\tilde{R}_j, A] &= iR_{lj}, & [A, R_{lj}] &= i\tilde{R}_j, & [A, S_{lj}] &= 0. \end{aligned} \quad (42)$$

The operators \mathbf{R}_l and $\tilde{\mathbf{R}}_l$ are orthogonal to \mathbf{S}_l in accordance with (5). Besides, $\mathbf{R}_l \cdot \tilde{\mathbf{R}}_l = 3X^{S_l S_r}$, and the Casimir operator is $\mathcal{K} = \mathbf{S}_l^2 + \mathbf{R}_l^2 + \tilde{\mathbf{R}}_l^2 + A^2 = 4$. The exchange tunneling Hamiltonian now reads

$$H_{\text{cot}} = J_l^T \mathbf{S}_l \cdot \mathbf{s} + J_l^{ST} \mathbf{R}_l \cdot \mathbf{s} + \alpha_r J_{lr} \tilde{\mathbf{R}} \cdot \mathbf{s}. \quad (43)$$

The system of scaling equations for the three coupling constants is

$$\begin{aligned} \frac{dj_1}{d \ln d} &= -[j_1^2 + j_2^2 + j_3^2], \\ \frac{dj_2}{d \ln d} &= -2j_1 j_2, \\ \frac{dj_3}{d \ln d} &= -2j_1 j_3. \end{aligned} \quad (44)$$

Here $j_1 = \rho_0 J_l^T, j_2 = \rho_0 J_l^{ST}, j_3 = \rho_0 \alpha_r J_{lr}$. Like (36), this system may be solved exactly, and its solution for

the Kondo temperature is

$$T_{K1} = \bar{D} \exp \left\{ -\frac{1}{j_1 + \sqrt{j_2^2 + j_3^2}} \right\}. \quad (45)$$

Upon increasing $\delta_l = \bar{E}_{Sl} - \bar{E}_{Tl}$ the energy E_{Sl} is quenched, and at $\delta_l \gg T_{K1}$ the symmetry gradually reduces to $SO(4)$, with Kondo temperature, $T_K = \delta_l \exp\{-[j_1(\delta_l) + j_3(\delta_l)]^{-1}\}$ (cf.¹⁵). On the other hand, upon decreasing $\delta_r = \bar{E}_{Tr} - \bar{E}_{Sl}$ the symmetry $P \times SO(4) \times SO(4)$ is restored at $\delta_r < T_{K0}$. The Kondo effect disappears when δ_l changes sign (the ground state becomes singlet).

The next asymmetric configuration is illustrated by the flow diagram of Fig. 5. In this case the manifold $\{T_l, S_l, T_r\}$ is involved in the dynamical symmetry of TQD. The relevant symmetry group is $SO(7)$. It is generated by six vectors and three scalars. These are spin operators \mathbf{S}_a ($a = l, r$) and R-operator \mathbf{R}_l (see Eq. 33) plus three vector operators $\tilde{\mathbf{R}}_i$ and three scalar operators A_i involving $l - r$ permutation. Here are the expressions for the spherical components of these vectors via Hubbard operators,

$$\begin{aligned} \tilde{R}_1^+ &= \sqrt{2}(X^{1_r 0_l} + X^{0_r \bar{1}_l}), & \tilde{R}_1^z &= X^{1_l 1_r} - X^{\bar{1}_r \bar{1}_l}, \\ \tilde{R}_2^+ &= \sqrt{2}(X^{1_l 0_r} + X^{0_r \bar{1}_l}), & \tilde{R}_2^z &= X^{1_r 1_l} - X^{\bar{1}_l \bar{1}_r}, \\ \tilde{R}_3^+ &= \sqrt{2}(X^{1_r S_l} - X^{S_l \bar{1}_r}), & \tilde{R}_3^z &= -(X^{0_r S_l} + X^{S_l 0_r}). \end{aligned} \quad (46)$$

The scalar operators A_1, A_2, A_3 are

$$\begin{aligned} A_1 &= \frac{i\sqrt{2}}{2} \left(X^{1_r \bar{1}_l} - X^{1_l \bar{1}_r + X^{\bar{1}_r 1_l} - X^{\bar{1}_l 1_r}} \right), \\ A_2 &= \frac{\sqrt{2}}{2} \left(X^{1_l \bar{1}_r} - X^{1_r \bar{1}_l} + X^{\bar{1}_r 1_l} - X^{\bar{1}_l 1_r} \right), \\ A_3 &= i(X^{0_l 0_r} - X^{0_r 0_l}). \end{aligned} \quad (47)$$

The (somewhat involved) commutation relations of o_7 algebra for these operators and various kinematic constraints are presented in Appendix C.

The SW transformation results in the effective cotunneling Hamiltonian

$$\begin{aligned} H_{\text{cot}} &= \sum_{a=l,r} J_{1a} \mathbf{S}_a \cdot \mathbf{s} + J_2 (\tilde{\mathbf{R}}_1 + \tilde{\mathbf{R}}_2) \cdot \mathbf{s} \\ &\quad + J_3 \tilde{\mathbf{R}}_3 \cdot \mathbf{s} + J_4 \mathbf{R}_l \cdot \mathbf{s}, \end{aligned} \quad (48)$$

where $J_{1a} = J_a^T, J_2 = J_{lr}, J_3 = \alpha_l J_{lr}$ and $J_4 = \alpha_l J_l^T$. The system of scaling equations for the Hamiltonian (48) has the form,

$$\begin{aligned} \frac{dj_{1l}}{d \ln d} &= -[j_{1l}^2 + j_2^2 + j_4^2], \\ \frac{dj_{1r}}{d \ln d} &= -[j_{1r}^2 + j_2^2 + j_3^2], \\ \frac{dj_2}{d \ln d} &= -[j_2(j_{1l} + j_{1r}) + j_3 j_4], \\ \frac{dj_3}{d \ln d} &= -2[j_{1r} j_3 + j_2 j_4], \\ \frac{dj_4}{d \ln d} &= -2[j_{1l} j_4 + j_2 j_3], \end{aligned} \quad (49)$$

where $j = \rho_0 J$. From Eqs. (49) the Kondo temperature is calculated,

$$T_K = \bar{D} \exp \left\{ -\frac{2}{j_+ + \sqrt{j_-^2 + \tilde{j}^2}} \right\}, \quad (50)$$

with

$$\begin{aligned} j_+ &= j_{1l} + j_{1r} + j_3 + j_4, \\ j_- &= j_{1l} + j_4 - j_{1r} - j_3, \\ \tilde{j} &= 2j_2 + j_3 + j_4. \end{aligned} \quad (51)$$

Like in the cases considered above, the Kondo temperature and the dynamical symmetry itself depend on the level splitting. On quenching the S_l state (increasing $\delta_{lr} = \bar{E}_{S_l} - \bar{E}_{T_r}$), the symmetry is changed for $P \times SO(3) \times SO(3)$ symmetry of two degenerate triplets with mirror reflection axis. Changing the sign of δ_{lr} one comes to a singlet regime with $T_K = 0$.

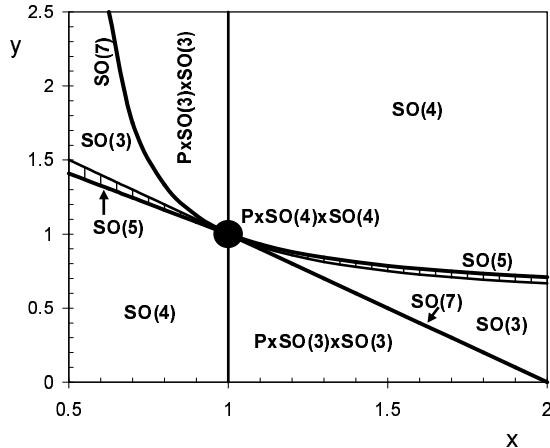


FIG. 6: Phase diagram of TQD. The Numerous dynamical symmetries of a TQD in the parallel geometry are presented in the plane of experimentally tunable parameters $x = \Gamma_l/\Gamma_r$ and $y = E_{lc}/E_{rc}$.

The results of calculations described in this subsection are summarized in Fig. 6. The central domain of size T_{K0} describes the fully symmetric state where there is left-right symmetry. Other regimes of Kondo tunneling correspond to lines or segments in the $\{x, y\}$ plane. These lines correspond to cases of higher conductance (ZBA). On the other hand, at some regions, the TQD has a singlet ground state and the Kondo effect is absent. These are marked by the vertically hatched domain. Both the tunneling rates which enter the ratio x and the relative level positions which determine the parameter y depend on the applied potentials, so the phase diagram presented in Fig. 6 can be scanned *experimentally* by appropriate variations of V_a and V_{ga} . This is a rare occasion where an abstract concept like dynamical symmetry can be felt and tuned by experimentalists. The quantity that is measured in tunneling experiments is the

zero-bias anomaly (ZBA) in tunnel conductance g .¹⁰ The ZBA peak is strongly temperature dependent, and this dependence is scaled by T_K . In particular, in a high temperature region $T > T_K$, where the scaling approach is valid, the conductance behaves as

$$g(T) \sim \ln^{-2}(T/T_K). \quad (52)$$

As it has been demonstrated above, T_K in CQD is a non-universal quantity due to partial break-down of dynamical symmetry in these quantum dots. It has a maximum value in the point of highest symmetry $P \times SO(4) \times SO(4)$, and depends on the parameters δ_a in the less symmetric phases (see, e.g., Eqs. 38, 39, 45, 50). Thus, scanning the phase diagram means changing $T_K(\delta_a)$. These changes are shown in Fig.7 which

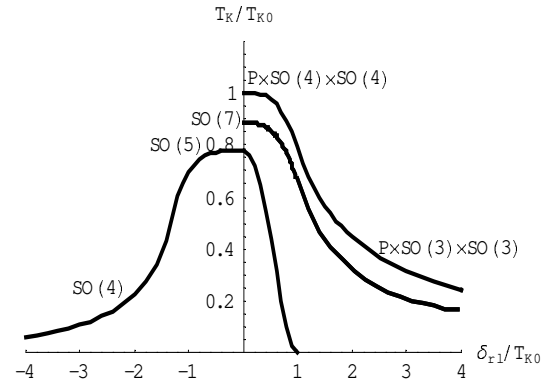


FIG. 7: Variation of Kondo temperature with $\delta_{rl} \equiv V_{gr} - V_{gl}$. Increasing this parameter removes some of the degeneracy and either "breaks" or reduces the corresponding dynamical symmetry.

illustrates the evolution of T_K with δ_{rl} for $x = 0.96, 0.8$ and 0.7 corresponding to a symmetry change from $P \times SO(4) \times SO(4)$, $SO(7)$ to $P \times SO(3) \times SO(3)$ and from $SO(5)$ to $SO(4)$, respectively. It is clear that the conductance measured at given T should follow variation of T_K in accordance with (52).

B. Odd occupation

We now turn our attention to an investigation of the dynamical symmetries of TQD with odd occupation $N = 3$, whose low-energy spin multiplet consists of two doublets and a quartet (23). Like in the four-electron case, the scaling equations (27) may be derived with different tunneling rates for different spin states (Γ_Q for the quartet and Γ_{D_i} ($i = 1, 2$) for the doublets).

$$\begin{aligned} \Gamma_Q &= \pi \rho_0 (V_l^2 + V_r^2), \\ \Gamma_{D_1} &= \gamma_1^2 \Gamma_Q, \quad \Gamma_{D_2} = \gamma_2^2 \Gamma_Q, \end{aligned} \quad (53)$$

with

$$\gamma_1 = \sqrt{1 - \frac{3}{2}(\beta_l^2 + \beta_r^2)}, \quad \gamma_2 = \sqrt{1 - \frac{1}{2}(\beta_l^2 + \beta_r^2)}. \quad (54)$$

Since $\Gamma_Q > \Gamma_{D_1}, \Gamma_{D_2}$, the scaling trajectories cross in a unique manner: This is the complete degenerate configuration where all three phase trajectories E_A intersect [$E_Q(D^*) = E_{D1}(D^*) = E_{D2}(D^*)$] at the same point D^* . This happens at bandwidth $D = D^*$ (Fig.8) whose value is estimated as

$$D_c^* = D_0 \exp \left(-\frac{\pi r}{\Gamma_Q} \right), \quad (55)$$

where

$$r = \frac{W_l^2 E_{rc} + W_r^2 E_{lc}}{W_l^2 E_{rc}^2 + W_r^2 E_{lc}^2} E_{lc} E_{rc}.$$

If this degenerate point occurs in the SW crossover re-

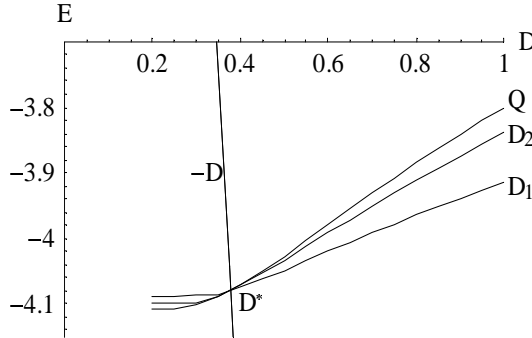


FIG. 8: Scaling trajectories resulting in $SO(4) \times SU(2)$ symmetry of TQD with $N = 3$.

gion, i.e., if $D^* \approx \bar{D}$, the SW procedure involves all three spin states, and it results in the following cotunneling Hamiltonian

$$H_{cot} = [J_{lr}^T \mathbf{S} + J_{lr}^{ST} \mathbf{R}] \cdot \mathbf{s}, \quad (56)$$

where \mathbf{S} is the spin 1 operator and \mathbf{R} is the R-operator describing S/T transition similar to that for spin rotator¹⁴. The coupling constants are

$$J_{lr}^T = \sum_{a=l,r} \frac{4\gamma_1 |V_a|^2}{3(\epsilon_F - \epsilon_a)}, \quad J_{lr}^{ST} = \gamma_2 J_{lr}^T. \quad (57)$$

This is a somewhat unexpected situation where Kondo tunneling in a quantum dot with *odd* occupation demonstrates the exchange Hamiltonian of a quantum dot with *even* occupation. The reason for this scenario is the specific structure of the wave function of TQD with $N = 3$. The corresponding wave functions $|\Lambda\rangle$ (see Appendix A) are vector sums of states composed of a "passive" electron sitting in the central dot and singlet/triplet (S/T) two-electron states in the l, r dots. Constructing the eigenstates $|\Lambda\rangle$ using certain Young tableaux (see Appendix D), one concludes that the spin dynamics of such TQD is represented by the spin 1 operator \mathbf{S} corresponding to the $l - r$ triplet, the corresponding R-operator \mathbf{R} and the spin 1/2 operator \mathbf{s}_c of a passive electron in the central

well. The latter does not enter the effective Hamiltonian H_{cot} (56) but influences the kinematic constraint via Casimir operator $\mathcal{K} = \mathbf{S}^2 + \mathbf{M}^2 + \mathbf{s}_c^2 = \frac{15}{4}$. The dynamical symmetry is therefore $SO(4) \times SU(2)$, and only the $SO(4)$ subgroup is involved in Kondo tunneling.

The scaling equations have the form,

$$\begin{aligned} \frac{dj_1}{d \ln d} &= -[j_1^2 + j_2^2], \\ \frac{dj_2}{d \ln d} &= -2j_1 j_2, \end{aligned} \quad (58)$$

where $j_1 = \rho_0 J_{lr}^T$, $j_2 = \rho_0 J_{lr}^{ST}$. From Eqs. (58) we obtain the Kondo temperature,

$$T_{K0} = \bar{D} \exp \left\{ -\frac{1}{j_1 + j_2} \right\}. \quad (59)$$

An additional dynamical symmetry arises in the case when $D^* > \bar{D}$. In this case the ground state of TQD is a quartet $S=3/2$, and we arrive at a standard underscreened Kondo effect for $SU(2)$ quantum dot as an ultimate limit of the above highly degenerate state.

C. Section summary

We have analyzed a couple of examples of TQD with even and odd occupation in the parallel geometry (Fig. 1). Actually, the metallic leads are represented by a single channel due to a unitary rotation in source-drain space. Our analysis demonstrate the principal features of Kondo effect in CQD in comparison with the conventional SQD composed of a single well. These examples teach us that in Kondo tunneling through CQD, not only the spin rotation but also Runge-Lenz operators \mathbf{R} and $\tilde{\mathbf{R}}$ are involved. Physically, the operators $\tilde{\mathbf{R}}$ describe left-right transitions, and different Young schemes give different spin operators in the effective co-tunneling Hamiltonians (see Appendix D). As a result, the nominal spin of CQD does not necessarily coincide with that involved in Kondo tunneling. A simple albeit striking realization of this scenario in this context is the case of TQD with $N = 3$, which manifests itself as a dot with integer or half-integer spin depending on gate voltages.

IV. ANISOTROPIC KONDO TUNNELING THROUGH TQD IN PARALLEL GEOMETRY

A. Generalities

In all examples of CQDs considered in the previous sections the co-tunneling problem is mapped on the specific spin Hamiltonian where both \mathbf{S} and \mathbf{R} vectors are involved in resonance cotunneling. There are, however, more exotic situations where the effective spin Hamiltonian is in fact a "Runge-Lenz" Hamiltonian in the sense

that the vectors \mathbf{R} *alone* are responsible for Kondo effect. Actually, just this aspect of dynamical symmetry in Kondo tunneling was considered in the theoretical papers cited in Ref. 6 and observed experimentally in Refs. 25, in which the Kondo effect in planar and vertical QDs induced by external magnetic field B has been observed. In this section we lay down the theoretical basis for this somewhat unusual kind of Kondo effect.

Consider again the case of TQD in parallel geometry with $N = 4$ discussed briefly in Ref. 15. In the previous sections the variation of spin symmetry arouse due to the interplay of two contributions to indirect exchange coupling between the spins \mathbf{S}_a . One source of such an exchange is tunneling within the CQD (amplitudes W_a) and another one is the tunneling between the dots and the leads (amplitudes V_a). Appropriate tuning of these two contributions results in occasional degeneracy of spin states (elimination of exchange splitting), and various combinations of these occasional degeneracies lead to the rich phase diagram presented in Fig. 6. A somewhat more crude, yet more compliant with experimental observation of such interplay is provided by the Zeeman effect. This mechanism is effective for CQD which remains in a singlet ground state after all exchange renormalizations have taken place. The negative exchange energy δ_a may then be compensated by the Zeeman splitting of the nearest triplet states, and Kondo effect arises once this compensation is complete⁶. From the point of view of dynamical symmetry, the degeneracy induced by magnetic field means realization of one possible subgroup of the non-compact group $SO(n)$ (see Eq. 21 and corresponding discussion in Section II). The transformation $SO(4) \rightarrow SU(2)$ for DQD in magnetic field was discussed in Ref.¹⁴.

B. Kondo effect in a non-magnetic sector

In similarity with DQD, the Kondo tunneling may be induced by external field B in the non-magnetic sector of the phase diagram of Fig. 6 close to $SO(5)$ line. Here the Zeeman splitting compensates negative $\delta_{l,r} = E_{S_{l,r}} - E_{T_{l,r}}$. The Kondo effect emerges when the Zeeman splitting energy $E_z = g\mu_B B \approx \delta_{l,r}$. Due to this compensation $E_{T1} \approx E_{S_{l,r}}$ and the spin Hamiltonian confined to this subspace has a form of *anisotropic* $SU(2)$ Kondo Hamiltonian

$$\tilde{H}_{\text{cot}} = J_{\parallel} R_z s_z + J_{\perp} (R^+ s^- + R^- s^+) / 2. \quad (60)$$

Here $J_{\parallel} = J_l^T$, $J_{\perp} = \sqrt{2[(\alpha_l J_l^T)^2 + (\alpha_r J_{lr})^2]}$. The vector \mathbf{R} is defined as,

$$R^+ = \sum_{a=l,r} F_a X^{1_l S_a}, \quad R^- = (R^+)^{\dagger}, \quad (61)$$

$$R_z = \frac{1}{2} \left[X^{1_l 1_l} - \sum_{a=l,r} (F_a^2 X^{S_a S_a} + F_a F_{\bar{a}} X^{S_a S_{\bar{a}}}) \right],$$

where $F_l = \sqrt{2}\alpha_l J_{\parallel} / J_{\perp}$, $F_r = \sqrt{2}\alpha_r J_{lr} / J_{\perp}$, $F_l^2 + F_r^2 = 1$, and $[R_j, R_k] = ie_{jkm} R_m$. The operators (61) generate the algebra o_3 in the spin subspace $\{T_{1_l}, S_l, S_r\}$ specified by the Casimir operator

$$R^2 = \frac{3}{4} \left[X^{1_l 1_l} + \sum_{a=l,r} (F_a^2 X^{S_a S_a} + F_a F_{\bar{a}} X^{S_a S_{\bar{a}}}) \right].$$

As was mentioned above the effective cotunneling Hamiltonian (60) contains solely the components of the \mathbf{R} -vectors. These vectors are prepared from the states of initial multiplet $\{T_{1_l}, S_l, S_r\}$ in a tricky manner: the $l-r$ symmetry is engaged in formation of longitudinal component R_z of the \mathbf{R} -vector (61).

The scaling equations for dimensionless exchange constants read,

$$\frac{dj_{\parallel}}{d \ln d} = -(j_{\perp})^2, \quad \frac{dj_{\perp}}{d \ln d} = -j_{\parallel} j_{\perp}, \quad (62)$$

yielding the unconventional expression for the Kondo temperature,

$$T_{Kz} = \bar{D} \exp \left[-\frac{1}{C_1} \left(\frac{\pi}{2} - \arctan \left(\frac{j_{\parallel}}{C_1} \right) \right) \right], \quad (63)$$

where $C_1 = \sqrt{(2\alpha_l^2 - 1)(j_{\parallel})^2 + 2(\alpha_r j_{lr})^2}$. Due to multi-branch nature of $\arctan(x)$ the RG flow diagram is rather complicated (see section 5.2.1 in Ref. 28), but the only stable fixed point is the strong-coupling solution $j_{\perp} = j_{\parallel} = \infty$. This implies that, somewhat unexpected, the Kondo-type ZBA in the conductance does occur at finite magnetic field.

Another type of field induced Kondo effect is realized in the symmetric case of $\delta = E_{S_{l,r}} - E_{T_{l,r}} < 0$. Now the Zeeman splitting compensates negative δ . Then two components of the triplets, namely $E_{T_{1_l,r}}$ cross with two singlet states $E_{S_{l,r}}$, and the symmetry group of the TQD in magnetic field is $SO(4)$. The o_4 algebra is formed by two vectors \mathbf{R}_1 and $\mathbf{R}_2 = \hat{P} \mathbf{R}_1$ which intermix the states $S_{l,r}$ and $T_{1_l,r}$,

$$R_1^+ = \sqrt{2}(X^{1_l S_l} + X^{1_r S_r}), \quad R_1^- = (R_1^+)^{\dagger},$$

$$R_{1z} = \frac{1}{2} \sum_{a=l,r} (X^{1_a 1_a} - X^{S_a S_a}),$$

$$R_2^+ = \sqrt{2}(X^{1_l S_r} + X^{1_r S_l}), \quad R_2^- = (R_2^+)^{\dagger},$$

$$R_{2z} = \frac{1}{2} \sum_{a=l,r} (X^{1_a 1_{\bar{a}}} - X^{S_a S_{\bar{a}}}), \quad (64)$$

The operators (64) obey the commutation relations of the o_4 algebra,

$$[R_{1j}, R_{1k}] = ie_{jkm} R_{1m},$$

$$[R_{2j}, R_{2k}] = ie_{jkm} R_{2m},$$

$$[R_{2j}, R_{1k}] = ie_{jkm} R_{2m}. \quad (65)$$

The Casimir operator in this case is $\mathbf{R}_1^2 + \mathbf{R}_2^2 = (3/2)$. The Kondo Hamiltonian is also anisotropic,

$$\tilde{H}_{cot} = J_1 \sum_{i=1,2} R_{iz} s_z + \frac{J_2}{2} \sum_{i=1,2} (R_i^+ s^- + R_i^- s^+) \quad (66)$$

where $J_1 = J^T$, $J_2 = \alpha J^T$. RG procedure similar to (62) yields the Kondo temperature

$$T_{Kz} = \bar{D} \exp \left[-\frac{1}{2C_2} \left(\frac{\pi}{2} - \arctan \left(\frac{j^T}{C_2} \right) \right) \right], \quad (67)$$

where $C_2 = \sqrt{(2\alpha^2 - 1)(j^T)^2}$.

C. Quantum dot with $SU(3)$ dynamical symmetry

A very peculiar Kondo tunneling is induced by an external magnetic field B in the non-magnetic sector of the phase diagram of Fig. 6 close to $SO(7)$ line. In this case the remarkable symmetry reduction occurs when the exchange splitting $\delta_l = E_{S_l} - E_{T_l} < 0$ and $\delta_{lr} = E_{S_l} - E_{T_r} < 0$ are equal and the Zeeman splitting compensates both of them simultaneously. Then we are left in a subspace $\{T_{1l}, S_l, T_{1r}\}$, and the interaction Hamiltonian has the form,

$$\begin{aligned} \tilde{H}_{cot} = & (J_{1l} R_l^z + J_{1r} R_r^z) s_z + J_2 (R_{lr} + R_{rl}) s_z \\ & + \frac{\sqrt{2}}{2} [(J_3 R_l^+ + J_4 R_r^+) s^- + (J_3 R_l^- + J_4 R_r^-) s^+] \end{aligned} \quad (68)$$

Here

$$\begin{aligned} J_{1l} &= \frac{2}{3} (2J_{1l}^T - J_{1r}^T), & J_{1r} &= \frac{2}{3} (2J_{1r}^T - J_{1l}^T), \\ J_2 &= J_{lr}, & J_3 &= \alpha_l J_{1l}^T, & J_4 &= \alpha_l J_{lr}. \end{aligned} \quad (69)$$

The operators \mathbf{R}_l , \mathbf{R}_r , R_{lr} and R_{rl} are defined as,

$$\begin{aligned} R_{az} &= \frac{1}{2} (X^{1_a 1_a} - X^{S_l S_l}), & (a &= l, r) \\ R_a^+ &= X^{1_a S_l}, & R_a^- &= (R_a^+)^{\dagger}, \\ R_{lr} &= X^{1_l 1_r}, & R_{rl} &= R_{lr}^{\dagger}. \end{aligned} \quad (70)$$

We see that the anisotropic Kondo Hamiltonian (68) is quite unconventional. There are several different terms responsible for transverse and longitudinal exchange involving the R-operators which generate both S/T_a and $T_a/T_{\bar{a}}$ transitions.

The operators (70) obey the following commutation relations,

$$\begin{aligned} [R_{aj}, R_{ak}] &= i e_{jkm} R_{am}, & [R_{aj}, R_{\bar{a}k}] &= \frac{i}{2} e_{jkm} R_{\bar{a}m}, \\ [R_{a\bar{a}}, R_{\bar{a}}^+] &= R_a^+, & [R_{a\bar{a}}, R_a^-] &= -R_{\bar{a}}^-, \\ [R_{lr}, R_{rl}] &= 2(R_{lz} - R_{rz}), & [R_{az}, R_{a\bar{a}}] &= 0. \end{aligned} \quad (71)$$

These operators generate the algebra u_3 in the reduced spin space $\{T_{1l}, S_l, T_{1r}\}$ specified by the Casimir operator

$$\mathbf{R}_l^2 + \mathbf{R}_r^2 + R_{lr}^2 + R_{rl}^2 = \frac{3}{2}.$$

Therefore, in this case the TQD possesses $SU(3)$ symmetry. These R operators may be represented via the familiar Gell-Mann matrices λ_i ($i = 1, \dots, 8$) for $SU(3)$ group,

$$\begin{aligned} R_l^+ &= \frac{1}{2} (\lambda_1 + i\lambda_2), & R_l^- &= \frac{1}{2} (\lambda_1 - i\lambda_2), \\ R_r^+ &= \frac{1}{2} (\lambda_6 - i\lambda_7), & R_r^- &= \frac{1}{2} (\lambda_6 + i\lambda_7), \\ R_{lz} &= \frac{1}{2} \lambda_3, & R_{rz} &= \frac{1}{4} (\lambda_3 - \sqrt{3}\lambda_8), \\ R_{lr} &= \frac{1}{2} (\lambda_4 + i\lambda_5), & R_{rl} &= \frac{1}{2} (\lambda_4 - i\lambda_5). \end{aligned}$$

As far as the RG procedure for the "Runge-Lenz" exchange Hamiltonian (68) the poor-man scaling procedure is applicable also for the R operators. The scaling equations have the form,

$$\begin{aligned} \frac{dj_{1l}}{d \ln d} &= -j_3^2, & \frac{dj_{1r}}{d \ln d} &= -j_4^2, & \frac{dj_2}{d \ln d} &= -j_3 j_4, \\ \frac{dj_3}{d \ln d} &= -[2j_{1l} j_3 + j_{1r} j_3 + j_2 j_4], \\ \frac{dj_4}{d \ln d} &= -[2j_{1r} j_4 + j_{1l} j_4 + j_2 j_3], \end{aligned} \quad (72)$$

where $j = \rho_0 J$. Eqs. (72) give the Kondo temperature,

$$T_{Kz} = \bar{D} \left(\frac{j_{1l} + j_{1r} + 2j_2 - C}{j_{1l} + j_{1r} + 2j_2 + C} \right)^{\frac{1}{2C}}, \quad (73)$$

where $C = \sqrt{(j_{1l} + j_{1r} + 2j_2)^2 - (j_3 + j_4)^2}$. Quite remarkably, in this case the Kondo temperature even loses its "conventional" exponential form, although the conventional result pertaining to infinite fixed point remains intact.

D. Section summary

We have found that the loss of rotational invariance in external magnetic field radically changes the dynamical symmetry of TQD. We considered here three examples of symmetry reduction, namely $SO(5) \rightarrow SU(2)$, $SO(5) \rightarrow SO(4)$ and $SO(7) \rightarrow SU(3)$. In all cases the Kondo exchange is anisotropic, which, of course, reflects the axial anisotropy induced by external field. All three cases as well as the $SO(4) \rightarrow SU(2)$ reduction considered earlier^{13,14} describe the magnetic field induced Kondo effect owing to the dynamical symmetry of complex quantum dots.

Although the anisotropic Kondo Hamiltonian was introduced formally at the early stage of Kondo physics²⁹, it is rather difficult to perceive how such Hamiltonian is derivable from the generic Anderson-type Hamiltonian. The effective anisotropy arises in cases, where the pseudo-spin degrees of freedom (like a two-level system) are responsible for anomalous scattering. Another possibility is the introduction of magnetic anisotropy in the generic spin Hamiltonian due to spin-orbit interaction (see Ref. 30 for a review of such models). One should also mention the remarkable possibility of magnetic field induced anisotropic Kondo effect on a magnetic impurity in ferromagnetic rare-earth metals with easy plane magnetic anisotropy³¹. This model is close to our model from the point of view of effective spin Hamiltonian, but the sources of anisotropy are different in the two systems. In our case the interplay between singlet and triplet components of spin multiplet is an eventual source both of Kondo effect itself and of its anisotropy in external magnetic field. Finally we pointed out a couple of interesting features. The first one is mainly appealing from the point of view that Symmetry is universal. Thus, $SU(3)$ appears in Particle Physics (quark color symmetry), in Nuclear Physics (Interacting Boson models) and now it has its place in Condensed Matter Physics³². The second one is rather novel. The result for T_K in expression (73) is apparently the first example in which the Kondo temperature is given as an *algebraic* function of the exchange constants.

V. TRIPLE QUANTUM DOT IN SERIES

A. Motivation

In SQD or in CQD arranged in the *parallel* geometry, the tunneling part of the bare Anderson Hamiltonian has the basic ingredient $(V_l c_{k\sigma l} + V_r c_{k\sigma r})d_{a\sigma}^{\dagger} + H.c.$. In other words, electron from the source and drain leads are coupled to the *same* dot electron. This enables a simple canonical transformation in source-drain space which eliminates the lead dependence¹². This is the reason why a quantum dot which, seemingly, has *two* sources of metallic electrons still cannot be mapped on a two-channel Kondo problem. We have recently shown that in a TQD in a series geometry such transformation cannot be constructed and elimination of channel index is therefore impossible³⁴. As a result the challenging situation arises in case of odd occupation $N = 3$, where the net spin of TQD is $S = 1/2$, and two leads play part of two channels in Kondo tunneling Hamiltonian. Unfortunately, despite the occurrence of two electron channels in the spin Hamiltonian, the complete mapping on the two-channel Kondo problem is not attained because there is an additional cotunneling term $J_{sd}\mathbf{S} \cdot \mathbf{s}_{sd} + H.c.$ (\mathbf{s}_{sd} is determined by (20)) which turns out to be relevant, and the two-channel fixed point cannot be reached. And yet, from the point of view of dynamical symmetry the series

geometry offers a new perspective which we analyze in the present section for the case of even occupation.

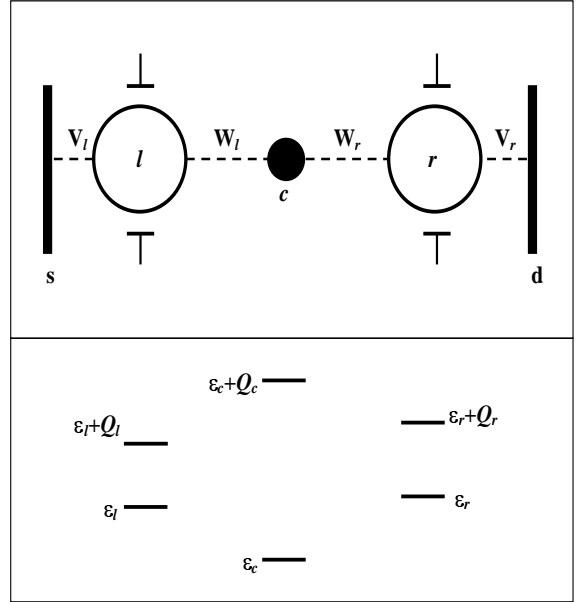


FIG. 9: Triple quantum dot in series. Left (l) and right (r) dots are coupled by tunneling $W_{l,r}$ to the central (c) dot and by tunneling $V_{l,r}$ to the source (s) and drain (d) leads.

B. Formalism and scaling equations

Consider then a TQD in series (Fig.9) with four electron occupation $N = 4$. The Hamiltonian of the system can be written in the form,

$$H = \sum_{\Lambda_a} E_{\Lambda_a} X^{\Lambda_a \Lambda_a} + \sum_{\lambda} E_{\lambda} X^{\lambda \lambda} + \sum_{k\sigma} \sum_{b=s,d} \epsilon_{kb} c_{k\sigma b}^{\dagger} c_{k\sigma b} + \sum_{\Lambda\lambda} \sum_{k\sigma} (V_{l\sigma}^{\lambda\Lambda} c_{k\sigma s}^{\dagger} X^{\lambda\Lambda} + V_{r\sigma}^{\lambda\Lambda} c_{k\sigma d}^{\dagger} X^{\lambda\Lambda} + H.c.), \quad (74)$$

where $|\Lambda\rangle$, $|\lambda\rangle$ are the four- and three-electron eigenfunctions (A5) and (A8); E_{Λ} , E_{λ} are the four- and three-electron energy levels (22) and (23), respectively; $X^{\lambda\Lambda} = |\lambda\rangle\langle\Lambda|$ are number changing dot Hubbard operators. The tunneling amplitudes $V_{a\sigma}^{\lambda\Lambda} = V_a \langle\lambda|d_{a\sigma}|\Lambda\rangle$ ($a = l, r$) depend explicitly on the respective 3 – 4 particle quantum numbers λ , Λ . Elimination of one of the two channels by the rotation (29) is then impossible since adding l or r electron to a given state λ results in different states Λ . Note that direct tunneling through the TQD is suppressed due to electron level mismatch and Coulomb blockade, so that only *cotunneling* mechanism contributes to the current.

Like in the parallel geometry case, the effective cotunneling Hamiltonian can be derived using Schrieffer-Wolf

procedure³³ (see Appendix B). To order $O(|V|^2)$, then,

$$\begin{aligned} H_{\text{cot}} = & \sum_{\Lambda_a} \bar{E}_{\Lambda_a} X^{\Lambda_a \Lambda_a} + \sum_{k\sigma} \sum_{b=s,d} \epsilon_{kb} c_{k\sigma b}^\dagger c_{k\sigma b} \\ & + \sum_{a=l,r} J_a^T \mathbf{S}_a \cdot \mathbf{s}_a + J_{sd} \hat{P} \sum_{a=l,r} \mathbf{S}_a \cdot \mathbf{s}_{a\bar{a}} \\ & + \sum_{a=l,r} J_a^{ST} \mathbf{R}_a \cdot \mathbf{s}_a + J_{sd} \sum_{a=l,r} \tilde{\mathbf{R}}_a \cdot \mathbf{s}_{\bar{a}a}. \quad (75) \end{aligned}$$

The antiferromagnetic coupling constants are defined by (31), (here we prefer the notation J_{sd} upon J_{lr} used in Eq.(31)). The vectors \mathbf{S}_a , \mathbf{R}_a and $\tilde{\mathbf{R}}_a$ are the dot operators (33), \hat{P} is the permutation operator (32). Here

$$\begin{aligned} \mathbf{s}_l &= \frac{1}{2} \sum_{kk'} \sum_{\sigma\sigma'} c_{k\sigma s}^\dagger \hat{\tau}_{\sigma\sigma'} c_{k'\sigma' s}, \\ \mathbf{s}_r &= \frac{1}{2} \sum_{kk'} \sum_{\sigma\sigma'} c_{k\sigma d}^\dagger \hat{\tau}_{\sigma\sigma'} c_{k'\sigma' d}, \\ \mathbf{s}_{lr} &= \frac{1}{2} \sum_{kk'} \sum_{\sigma\sigma'} c_{k\sigma s}^\dagger \hat{\tau}_{\sigma\sigma'} c_{k'\sigma' d}, \quad \mathbf{s}_{rl} = (\mathbf{s}_{lr})^\dagger, \end{aligned}$$

notation is used instead of (20). The vector operators \mathbf{S}_a , \mathbf{R}_a , $\tilde{\mathbf{R}}_a$ and the permutation operator \hat{P} manifest the dynamical symmetry of the TQD. Unlike (30) the Hamiltonian (75) contains the non-diagonal tunneling terms $J_{sd} \hat{P} \sum_{a=l,r} \mathbf{S}_a \cdot \mathbf{s}_{a\bar{a}}$ and $J_{sd} \sum_{a=l,r} \tilde{\mathbf{R}}_a \cdot \mathbf{s}_{\bar{a}a}$ which cannot be excluded by the rotation (29).

Now we discuss possible realization of $P \times SO(4) \times SO(4)$ and $SO(5)$ symmetries arising in the TQD. The most symmetric case is realized when $E_{lc} = E_{rc}$ and $\Gamma_{T_r} = \Gamma_{T_l}$. If all four phase trajectories $E_\Lambda(D)$ intersect at $D = D_c$ (Fig. 3), the symmetry of the TQD is $P \times SO(4) \times SO(4)$. When $\alpha_l = \alpha_r = \alpha$ the operator $\tilde{\mathbf{R}}_l + \tilde{\mathbf{R}}_r$ transforms into $\hat{P}(\mathbf{R}_l + \mathbf{R}_r)$, and the exchange part of the Hamiltonian (75) reduces to

$$\begin{aligned} H_{\text{cot}} = & J^T \sum_a \mathbf{S}_a \cdot \mathbf{s}_a + J_{sd} \hat{P} \sum_a \mathbf{S}_a \cdot \mathbf{s}_{a\bar{a}} \\ & + J^{ST} \sum_a \mathbf{R}_a \cdot \mathbf{s}_a + \alpha J_{sd} \hat{P} \sum_a \mathbf{R}_a \cdot \mathbf{s}_{a\bar{a}}. \quad (76) \end{aligned}$$

The vector operators \mathbf{R}_a and \mathbf{S}_a obey the commutation relations (35) of o_4 Lie algebra.

After first step of RG procedure the interaction Hamiltonian (76) reads,

$$\begin{aligned} H_{\text{cot}} = & J_1^T \sum_a \mathbf{S}_a \cdot \mathbf{s}_a + J_1^{ST} \sum_a \mathbf{R}_a \cdot \mathbf{s}_a \\ & + J_2^T \hat{P} \sum_a \mathbf{S}_a \cdot \mathbf{s}_{a\bar{a}} + J_2^{ST} \hat{P} \sum_a \mathbf{R}_a \cdot \mathbf{s}_{a\bar{a}} \\ & + J_3^T \sum_a \mathbf{S}_a \cdot \mathbf{s}_{\bar{a}} + J_3^{ST} \sum_a \mathbf{R}_a \cdot \mathbf{s}_{\bar{a}}, \quad (77) \end{aligned}$$

where $J_1^T(\bar{D}) = J_2^T(\bar{D}) = J^T$, $J_3^T(\bar{D}) = 0$ and $J_i^{ST}(\bar{D}) = \alpha J_i^T(\bar{D})$ ($i = 1, 2, 3$).

The scaling equations are

$$\begin{aligned} \frac{dj_1^T}{d \ln d} &= - \left[(j_1^T)^2 + (j_1^{ST})^2 + \frac{(j_2^T)^2}{2} + \frac{(j_2^{ST})^2}{2} \right], \\ \frac{dj_2^T}{d \ln d} &= - [j_1^T j_2^T + j_1^{ST} j_2^{ST} + j_2^T j_3^T + j_2^{ST} j_3^{ST}], \\ \frac{dj_3^T}{d \ln d} &= - \left[(j_3^T)^2 + (j_3^{ST})^2 + \frac{(j_2^T)^2}{2} + \frac{(j_2^{ST})^2}{2} \right], \\ \frac{dj_1^{ST}}{d \ln d} &= - [2j_1^T j_1^{ST} + j_2^T j_2^{ST}], \\ \frac{dj_2^{ST}}{d \ln d} &= - [j_1^T j_2^{ST} + j_1^{ST} j_2^T + j_3^T j_2^{ST} + j_2^T j_3^{ST}], \\ \frac{dj_3^{ST}}{d \ln d} &= - [2j_3^T j_3^{ST} + j_2^T j_2^{ST}], \quad (78) \end{aligned}$$

where $j_i^T = \rho_0 J_i^T$, $j_i^{ST} = \rho_0 J_i^{ST}$ ($i = 1, 2, 3$). Equations (78) can be solved exactly and the solution gives the Kondo temperature

$$T_{K0} = \bar{D} \exp \left(- \frac{2}{(\sqrt{3}+1)(j_1^T + j_1^{ST})} \right). \quad (79)$$

Note that in the series geometry the scaling equations for the symmetry group $P \times SO(4) \times SO(4)$ are much more involved than those obtained in the parallel geometry for the same symmetry group (compare equations (36)).

When $\bar{E}_{S_l} \approx \bar{E}_{T_l} \approx \bar{E}_{S_r} < \bar{E}_{T_r}$ (Fig. 4), the TQD possess the $SO(5)$ symmetry. In this case the interaction Hamiltonian has the form

$$H_{\text{cot}} = J_1 \mathbf{S}_l \cdot \mathbf{s}_l + J_2 \mathbf{R}_l \cdot \mathbf{s}_l + J_3 (\tilde{\mathbf{R}}_1 \cdot \mathbf{s}_{lr} + \tilde{\mathbf{R}}_2 \cdot \mathbf{s}_{rl}) \quad (80)$$

where $J_1 = J_{1l}^T$, $J_2 = J_{1l}^{ST}$ and $J_3 = \alpha_r J_{sd}$. The spherical components of the vector operators $\tilde{\mathbf{R}}_1$ and $\tilde{\mathbf{R}}_2$ are given by the following expressions,

$$\begin{aligned} \tilde{R}_1^+ &= -\sqrt{2} X^{S_r \bar{1}_l}, \quad \tilde{R}_1^- = \sqrt{2} X^{S_r 1_l}, \quad \tilde{R}_{1z} = -X^{S_r 0_l}, \\ \tilde{R}_2^+ &= (\tilde{R}_1^-)^\dagger, \quad \tilde{R}_2^- = (\tilde{R}_1^+)^*, \quad \tilde{R}_{2z} = \tilde{R}_{1z}^\dagger. \quad (81) \end{aligned}$$

The operators \mathbf{S}_l , \mathbf{R}_l , $\tilde{\mathbf{R}} \equiv \tilde{\mathbf{R}}_1 + \tilde{\mathbf{R}}_2$ and A (41) generate the algebra o_5 in a representation specified by the Casimir operator $\mathcal{K} = \mathbf{S}_l^2 + \mathbf{R}_l^2 + \tilde{\mathbf{R}}^2 + A^2 = 4$.

After first step of RG procedure the interaction Hamiltonian (80) takes the form

$$\begin{aligned} H_{\text{cot}} = & J_1 \mathbf{S}_l \cdot \mathbf{s}_l + J_2 \mathbf{R}_l \cdot \mathbf{s}_l \\ & + J_3 (\tilde{\mathbf{R}}_1 \cdot \mathbf{s}_{lr} + \tilde{\mathbf{R}}_2 \cdot \mathbf{s}_{rl}) + J_4 \mathbf{S}_l \cdot \mathbf{s}_r, \quad (82) \end{aligned}$$

where $J_4(\bar{D}) = 0$.

The scaling equations have the form

$$\begin{aligned} \frac{dj_1}{d \ln d} &= - \left[j_1^2 + j_2^2 + \frac{j_3^2}{2} \right], \\ \frac{dj_2}{d \ln d} &= -2j_1 j_2, \\ \frac{dj_3}{d \ln d} &= -j_3(j_1 + j_4), \\ \frac{dj_4}{d \ln d} &= - \left[j_4^2 + \frac{j_3^2}{2} \right], \quad (83) \end{aligned}$$

where $j_i = \rho_0 J_i$ ($i = 1, \dots, 4$). Equations (83) gives the Kondo temperature

$$T_K = \bar{D} \exp \left\{ -\frac{2}{j_1 + j_2 + \sqrt{(j_1 + j_2)^2 + 2j_3^2}} \right\}. \quad (84)$$

Note the difference between the Kondo temperature with $SO(5)$ symmetry in the parallel geometry (see equation (45)) and the series geometry, equation (84) above.

C. Section summary

To conclude this section, the difference between the parallel and series geometry of a TQD has been clarified from the point of view of dynamical symmetries. It might be useful here to underscore the following two points: 1) An application of an external magnetic field leads here to various $SU(n)$ dynamical symmetries. We do not enter here the details of calculation, which follows the pattern of Section IV. These calculations show, in particular, that close (but not at) the symmetry point (see figure 6), the magnetic field leads to the symmetry group $P \times SU(2) \times SU(2)$, while near the $SO(5)$ line it leads to the symmetry group $SU(3)$. 2) In the case of odd electron occupation ($N = 3$) when the ground-state of the isolated TQD is a doublet and higher spin excitations can be neglected, the effective low-energy Hamiltonian of a TQD in series manifests a two-channel Kondo problem albeit *only in the weak coupling regime*³⁴. To describe the flow diagram in this case, one should go beyond the one-loop approximation in RG flow equations³⁵.

VI. CONCLUSIONS

We have analyzed the occurrence of dynamical symmetries in complex quantum dots. These symmetries emerge when the dot is coupled with metallic electrons under the conditions of strong Coulomb blockade and nearly degenerate low energy spin spectrum. It can be achieved either by an application of an external magnetic field or due to dot-lead tunneling which, as we have seen, results in level renormalization and the emergence of an additional symmetry. Although the main focus in this paper is related to the study of triple quantum dot, the generalization to other quantum dot structures is indeed straightforward.

Since we were interested in a symmetry aspect of Kondo tunneling Hamiltonian, we restricted ourselves by derivation of RG flow equations and solving them for Kondo temperature. In all cases the TQDs possess strong coupling fixed point characteristic for spin 1/2 and/or spin 1 case. We did not calculate the tunnel conductance in details, because it reproduces the main features of Kondo-type zero bias anomalies studied multiply by many authors (see, e.g.,^{6,12,13,14,15,22,23}). The novel feature is the possibility of changing T_K by scanning the

phase diagram of Fig. 6. Then the zero bias anomaly follows all symmetry crossovers induced by experimentally tunable gate voltages and tunneling rates.

The main message of our work is that symmetry enters the realm of mesoscopic physics in a rather non-trivial manner. Dynamical symmetry in this context is not just a geometrical concept but, rather, intimately related with the physics of strong correlations and exchange interactions. The relation with other branches of physics makes it even more attractive. The groups $SO(n)$ play an important role in Particle Physics as well as in model building for high temperature superconductivity (especially $SO(5)$). The role of the group $SU(3)$ in Particle Physics cannot be overestimated and its role in Nuclear Physics in relation with the interacting Boson model is well recognized. This paper extends the role of these Lie groups in Condensed Matter Physics.

Acknowledgement: This work is partially supported by grants from the Israeli Science Foundations and the United States Israel Binational Science Foundation.

APPENDIX A: DIAGONALIZATION OF THE DOT HAMILTONIAN

Here we describe the diagonalization procedure of the Hamiltonian of the isolated TQDs occupied by four and three electrons. The dot Hamiltonian has the form,

$$H_d = \sum_{a=l,r,c} \sum_{\sigma} \epsilon_a d_{a\sigma}^\dagger d_{a\sigma} + \sum_a Q_a n_{a\uparrow} n_{a\downarrow} + \sum_{a=l,r} (W_a d_{c\sigma}^\dagger d_{a\sigma} + H.c.). \quad (A1)$$

(a) Four electron occupation:

The Hamiltonian (A1) can be diagonalized by using the basis of four-electron wave functions

$$\begin{aligned} |t_a, 1\rangle &= d_{c\uparrow}^\dagger d_{a\uparrow}^\dagger d_{\bar{a}\uparrow}^\dagger d_{\bar{a}\downarrow}^\dagger |0\rangle, & |t_a, \bar{1}\rangle &= d_{c\downarrow}^\dagger d_{a\downarrow}^\dagger d_{\bar{a}\uparrow}^\dagger d_{\bar{a}\downarrow}^\dagger |0\rangle, \\ |t_a, 0\rangle &= \frac{1}{\sqrt{2}} (d_{c\uparrow}^\dagger d_{a\downarrow}^\dagger + d_{c\downarrow}^\dagger d_{a\uparrow}^\dagger) d_{\bar{a}\uparrow}^\dagger d_{\bar{a}\downarrow}^\dagger |0\rangle, \\ |s_a\rangle &= \frac{1}{\sqrt{2}} (d_{c\uparrow}^\dagger d_{a\downarrow}^\dagger - d_{c\downarrow}^\dagger d_{a\uparrow}^\dagger) d_{\bar{a}\uparrow}^\dagger d_{\bar{a}\downarrow}^\dagger |0\rangle, \\ |ex\rangle &= d_{l\uparrow}^\dagger d_{l\downarrow}^\dagger d_{r\uparrow}^\dagger d_{r\downarrow}^\dagger |0\rangle, \end{aligned} \quad (A2)$$

where $a = l, r$; $\bar{l} = r$, $\bar{r} = l$. The Coulomb interaction quenches the states with two electrons in the central dot and we do not take them into account. The states (A2) form a basis of two triplet and three singlet states. In this basis, the Hamiltonian (A1) is decomposed into triplet and singlet matrices,

$$H_t = \begin{pmatrix} \tilde{\epsilon}_l & 0 \\ 0 & \tilde{\epsilon}_r \end{pmatrix}, \quad (A3)$$

and

$$H_s = \begin{pmatrix} \tilde{\epsilon}_l & 0 & \sqrt{2}W_l \\ 0 & \tilde{\epsilon}_r & \sqrt{2}W_r \\ \sqrt{2}W_l & \sqrt{2}W_r & \tilde{\epsilon}_{ex} \end{pmatrix}, \quad (A4)$$

where $\tilde{\varepsilon}_l = \epsilon_c + \epsilon_l + 2\epsilon_r + Q_r$, $\tilde{\varepsilon}_r = \epsilon_c + \epsilon_r + 2\epsilon_l + Q_l$, and $\tilde{\varepsilon}_{ex} = 2\epsilon_l + 2\epsilon_r + Q_l + Q_r$. The eigenfunctions corresponding to the energy levels (22) are

$$\begin{aligned} |S_a\rangle &= \sqrt{1 - 2\beta_a^2} |s_a\rangle - \sqrt{2}\beta_a |ex\rangle, \\ |T_a\rangle &= |t_a\rangle, \\ |Ex\rangle &= \sqrt{1 - 2\beta_l^2 - 2\beta_r^2} |ex\rangle + \sqrt{2}\beta_l |s_l\rangle + \sqrt{2}\beta_r |s_r\rangle, \end{aligned} \quad (\text{A5})$$

where β_a are defined by Eq.(15).

(b) Three electron occupation:

In this case the Hamiltonian (A1) can be diagonalized by using the basis of three-electron wave functions

$$\begin{aligned} |d, \sigma\rangle &= \frac{([d_{c\uparrow}^+ d_{l\downarrow}^+ - d_{c\downarrow}^+ d_{l\uparrow}^+] d_{r\sigma}^+ + [d_{c\downarrow}^+ d_{r\uparrow}^+ - d_{c\uparrow}^+ d_{r\downarrow}^+] d_{l\sigma}^+) |0\rangle}{\sqrt{6}}, \\ |d_c, \sigma\rangle &= -\frac{1}{\sqrt{2}} (d_{l\uparrow}^+ d_{r\downarrow}^+ - d_{l\downarrow}^+ d_{r\uparrow}^+) d_{c\sigma}^+ |0\rangle, \\ \left|q, \pm \frac{3}{2}\right\rangle &= d_{c\pm}^+ d_{r\pm}^+ d_{l\pm}^+ |0\rangle, \\ \left|q, \pm \frac{1}{2}\right\rangle &= \frac{(d_{c\pm}^+ d_{r\pm}^+ d_{l\mp}^+ + d_{c\pm}^+ d_{r\mp}^+ d_{l\pm}^+ + d_{c\mp}^+ d_{r\pm}^+ d_{l\pm}^+) |0\rangle}{\sqrt{3}}, \\ |d_{lc}, \sigma\rangle &= d_{l\uparrow}^+ d_{l\downarrow}^+ d_{c\sigma}^+ |0\rangle, \quad |d_{rc}, \sigma\rangle = d_{r\uparrow}^+ d_{r\downarrow}^+ d_{c\sigma}^+ |0\rangle, \\ |d_l, \sigma\rangle &= d_{r\uparrow}^+ d_{r\downarrow}^+ d_{l\sigma}^+ |0\rangle, \quad |d_r, \sigma\rangle = d_{l\uparrow}^+ d_{l\downarrow}^+ d_{r\sigma}^+ |0\rangle, \quad (\text{A6}) \end{aligned}$$

where $\sigma = \uparrow, \downarrow$. The three-electron states $|\Lambda\rangle$ of the TQD are classified as a ground state doublet $|D_1\rangle$, low-lying doublet $|D_2\rangle$ and quartet $|Q\rangle$ excitations, and four charge-transfer excitonic doublets D_{ac} and D_a ($a = l, r$).

In the framework of second order perturbation theory with respect to β_a (15), the energy levels E_Λ are

$$\begin{aligned} E_{D_1} &= \epsilon_c + \epsilon_l + \epsilon_r - \frac{3}{2} [W_l \beta_l + W_r \beta_r], \\ E_{D_2} &= \epsilon_c + \epsilon_l + \epsilon_r - \frac{1}{2} [W_l \beta_l + W_r \beta_r], \\ E_Q &= \epsilon_c + \epsilon_l + \epsilon_r, \\ E_{D_{ac}} &= \epsilon_c + 2\epsilon_a + Q_a - W_{\bar{a}} \beta_{\bar{a}}, \\ E_{D_a} &= \epsilon_a + 2\epsilon_{\bar{a}} + Q_{\bar{a}} + W_a \beta_a + 2W_{\bar{a}} \beta_{\bar{a}}. \quad (\text{A7}) \end{aligned}$$

The eigenfunctions corresponding to the energy levels

(A7) are the following combinations,

$$\begin{aligned} |D_1, \sigma\rangle &= \gamma_1 |d_1, \sigma\rangle - \frac{\sqrt{6}}{2} \beta_l |d_r, \sigma\rangle + \frac{\sqrt{6}}{2} \beta_r |d_l, \sigma\rangle, \\ |D_2, \sigma\rangle &= \gamma_2 |d_2, \sigma\rangle - \frac{\sqrt{2}}{2} \beta_l |d_r, \sigma\rangle - \frac{\sqrt{2}}{2} \beta_r |d_l, \sigma\rangle, \\ |Q, s_z\rangle &= |q, s_z\rangle, \quad s_z = \pm \frac{3}{2}, \pm \frac{1}{2}, \\ |D_{ac}, \sigma\rangle &= \sqrt{1 - \beta_{\bar{a}}^2} |d_{ac}, \sigma\rangle - \beta_{\bar{a}} |d_{\bar{a}}, \sigma\rangle, \\ |D_r, \sigma\rangle &= \sqrt{1 - 2\beta_l^2 - \beta_r^2} |d_r, \sigma\rangle + \beta_r |d_{lc}, \sigma\rangle \\ &\quad + \frac{\sqrt{2}}{2} \beta_l (\sqrt{3} |d_1, \sigma\rangle + |d_2, \sigma\rangle), \\ |D_l, \sigma\rangle &= \sqrt{1 - 2\beta_r^2 - \beta_l^2} |d_l, \sigma\rangle + \beta_l |d_r, c, \sigma\rangle \\ &\quad - \frac{\sqrt{2}}{2} \beta_r (\sqrt{3} |d_1, \sigma\rangle - |d_2, \sigma\rangle), \end{aligned} \quad (\text{A8})$$

where γ_1 and γ_2 are determined by Eq.(54).

APPENDIX B: EFFECTIVE SPIN HAMILTONIAN

The spin Hamiltonian of the TQD with $N = 4$ occupation in parallel geometry (Fig.1) is derived below. The Hamiltonian of the system can be written in the form,

$$\begin{aligned} H &= \sum_{\Lambda} E_{\Lambda} X^{\Lambda\Lambda} + \sum_{\lambda} E_{\lambda} X^{\lambda\lambda} + \sum_{k\sigma} \epsilon_k c_{k\sigma}^+ c_{k\sigma} \\ &\quad + \sum_{\Lambda\lambda} \sum_{k\sigma, a} (V_{a\sigma}^{\lambda\Lambda} c_{k\sigma}^+ X^{\lambda\Lambda} + H.c.), \end{aligned} \quad (\text{B1})$$

where $|\Lambda\rangle$, $|\lambda\rangle$ are four- and three-electron eigenfunctions (A5) and (A8); E_{Λ} , E_{λ} are the four- and three-electron energy levels (22) and (23), respectively; $V_{a\sigma}^{\lambda\Lambda} = V_a \langle \lambda | d_{a\sigma} | \Lambda \rangle$ ($a = l, r$) and $X^{\lambda\Lambda} = |\lambda\rangle\langle\Lambda|$ are Hubbard operators.

The Schrieffer-Wolff transformation³³ for the configuration of four electron states of the molecule projects out the three electron states $|\lambda\rangle$ and maps the Hamiltonian (B1) onto an effective spin Hamiltonian \tilde{H} acting in a subspace of four-electron configurations $\langle\Lambda| \dots |\Lambda'\rangle$,

$$\tilde{H} = e^{i\mathcal{S}} H e^{-i\mathcal{S}} = H + \sum_m \frac{(i)^m}{m!} [\mathcal{S}, [\mathcal{S}, \dots [\mathcal{S}, H]] \dots] \quad (\text{B2})$$

where

$$\mathcal{S} = -i \sum_{\Lambda\lambda} \sum_{\langle k \rangle \sigma, a} \frac{V_{a\sigma}^{\Lambda\Lambda}}{E_{\Lambda\lambda} - \epsilon_k} X^{\Lambda\Lambda} c_{k\sigma} + h.c. \quad (\text{B3})$$

Here $\langle k \rangle$ stands for the electron or hole states secluded within a layer $\pm \bar{D}$ around the Fermi level. $\bar{E}_{\Lambda\lambda} = E_{\Lambda}(\bar{D}) - E_{\lambda}(\bar{D})$. The effective Hamiltonian with the

three-electron states $|\lambda\rangle$ frozen out can be obtained within first order in \mathcal{S} . It has the following form,

$$\begin{aligned}\tilde{H} &= \sum_{\Lambda} \bar{E}_{\Lambda} X^{\Lambda\Lambda} + \sum_{\langle k \rangle \sigma} \epsilon_k c_{k\sigma}^+ c_{k\sigma} \\ &- \sum_{\Lambda\Lambda' \lambda} \sum_{kk' \sigma\sigma'} \sum_{a=l,r} J_{kk',a\sigma}^{\Lambda\Lambda'} X^{\Lambda\Lambda'} c_{k\sigma}^+ c_{k'\sigma'},\end{aligned}\quad (\text{B4})$$

where

$$J_{kk',a\sigma}^{\Lambda\Lambda'} = (V_{a\sigma}^{\lambda\Lambda})^* V_{a\sigma'}^{\lambda'\Lambda} \left(\frac{1}{\bar{E}_{\Lambda\lambda} - \epsilon_k} + \frac{1}{\bar{E}_{\Lambda'\lambda} - \epsilon_{k'}} \right) \quad (\text{B5})$$

The constraint $\sum_{\Lambda} X^{\Lambda\Lambda} = 1$ is valid. Unlike the conventional case of doublet spin 1/2 we have here an octet $\Lambda = \{\Lambda_l, \Lambda_r\} = \{S_l, T_l, S_r, T_r\}$, and the SW transformation *intermixes all these states*. The effective spin Hamiltonian (B4) to order $O(|V|^2)$ acquires the form of Eq.(30).

APPENDIX C: SO(7) SYMMETRY

The operators \mathbf{S}_l , \mathbf{S}_r , \mathbf{R}_l , $\tilde{\mathbf{R}}_1$, $\tilde{\mathbf{R}}_2$, $\tilde{\mathbf{R}}_3$ and A_i ($i = 1, 2, 3$) (see Eqs.(33),(46),(47)) obey the commutation re-

lations of the o_7 Lie algebra,

$$[S_{aj}, S_{a'k}] = ie_{jkm} \delta_{aa'} S_{am}, \quad [R_{lj}, R_{lk}] = ie_{jkm} S_{lm},$$

$$[R_{lj}, S_{lk}] = ie_{jkm} R_{lm}, \quad [R_{lj}, S_{rk}] = [\tilde{R}_{3j}, S_{lk}] = 0,$$

$$[\tilde{R}_{3j}, \tilde{R}_{3k}] = ie_{jkm} S_{rm}, \quad [\tilde{R}_{3j}, S_{rk}] = ie_{jkm} \tilde{R}_{3m},$$

$$\begin{aligned}[\tilde{R}_{1j}, \tilde{R}_{1k}] &= ie_{jkm} S_{rm} (1 - \delta_{jz}) (1 - \delta_{kz}) \\ &+ \frac{i}{2} e_{jkm} S_{lm} (\delta_{jz} + \delta_{kz}) - \frac{1}{2} (S_{lj} \delta_{kz} - S_{lk} \delta_{jz}),\end{aligned}$$

$$\begin{aligned}[\tilde{R}_{2j}, \tilde{R}_{2k}] &= ie_{jkm} S_{lm} (1 - \delta_{jz}) (1 - \delta_{kz}) \\ &+ \frac{i}{2} e_{jkm} S_{rm} (\delta_{jz} + \delta_{kz}) - \frac{1}{2} (S_{rj} \delta_{kz} - S_{rk} \delta_{jz}),\end{aligned}$$

$$\begin{aligned}[\tilde{R}_{1j}, \tilde{R}_{2k}] &= \frac{i}{2} e_{jkm} (S_{rm} \delta_{jz} + S_{lm} \delta_{kz}) \\ &+ \frac{1}{2} [S_{lj} \delta_{kz} - S_{rk} \delta_{jz} + (S_{lz} - S_{rz}) \delta_{jz} \delta_{kz}],\end{aligned}$$

$$\begin{aligned}[\tilde{R}_{3j}, \tilde{R}_{1k}] &= ie_{jkm} R_{lm} (1 - \delta_{jz} - \frac{\delta_{kz}}{2}) \\ &- \frac{\delta_{kz}}{2} (1 - \delta_{jz}) R_{lj},\end{aligned}$$

$$[\tilde{R}_{3j}, \tilde{R}_{2k}] = ie_{jkm} R_{lm} (\delta_{jz} + \frac{\delta_{kz}}{2}) + \frac{\delta_{kz}}{2} (1 - \delta_{jz}) R_{lj},$$

$$[\tilde{R}_{1j}, R_{lk}] = ie_{jkm} \tilde{R}_{3m} (\delta_{kz} + \frac{\delta_{jz}}{2}) - \frac{\delta_{jz}}{2} (1 - \delta_{kz}) \tilde{R}_{3k},$$

$$\begin{aligned}[\tilde{R}_{2j}, R_{lk}] &= ie_{jkm} \tilde{R}_{3m} (1 - \delta_{kz} - \frac{\delta_{jz}}{2}) \\ &+ \frac{\delta_{jz}}{2} (1 - \delta_{kz}) \tilde{R}_{3k},\end{aligned}$$

$$[A_1, S_{lj}] = i A_2 \delta_{jz} + \frac{i\sqrt{2}}{2} (\tilde{R}_{1x} \delta_{jx} - \tilde{R}_{1y} \delta_{jy}),$$

$$[A_2, S_{lj}] = -i A_1 \delta_{jz} - \frac{i\sqrt{2}}{2} (\tilde{R}_{1y} \delta_{jx} + \tilde{R}_{1x} \delta_{jy}),$$

$$[A_1, S_{rj}] = i A_2 \delta_{jz} - \frac{i\sqrt{2}}{2} (\tilde{R}_{2x} \delta_{jx} - \tilde{R}_{2y} \delta_{jy}),$$

$$[A_2, S_{rj}] = -i A_1 \delta_{jz} + \frac{i\sqrt{2}}{2} (\tilde{R}_{2y} \delta_{jx} + \tilde{R}_{2x} \delta_{jy}),$$

$$[A_3, S_{lj}] = -i \tilde{R}_{2j} (1 - \delta_{jz}), \quad [A_3, S_{rj}] = i \tilde{R}_{1j} (1 - \delta_{jz}),$$

$$[A_1, R_{lj}] = -\frac{i\sqrt{2}}{2} (\tilde{R}_{3x} \delta_{jx} - \tilde{R}_{3y} \delta_{jy}),$$

$$[A_2, R_{lj}] = \frac{i\sqrt{2}}{2} (\tilde{R}_{3y} \delta_{jx} + \tilde{R}_{3x} \delta_{jy}),$$

$$[A_1, \tilde{R}_{3j}] = \frac{i\sqrt{2}}{2} (R_{lx} \delta_{jx} - R_{ly} \delta_{jy}),$$

$$[A_2, \tilde{R}_{3j}] = -\frac{i\sqrt{2}}{2} (R_{ly} \delta_{jx} + R_{lx} \delta_{jy}),$$

$$[A_3, R_{lj}] = -i \tilde{R}_{3z} \delta_{jz}, \quad [A_3, \tilde{R}_{3j}] = i R_{lz} \delta_{jz},$$

$$[A_1, \tilde{R}_{1j}] = -\frac{i\sqrt{2}}{2} (S_{lx} \delta_{jx} - S_{ly} \delta_{jy}),$$

$$[A_2, \tilde{R}_{1j}] = \frac{i\sqrt{2}}{2} (S_{ly} \delta_{jx} + S_{lx} \delta_{jy}),$$

$$[A_3, \tilde{R}_{1j}] = -i (S_{rx} \delta_{jx} + S_{ry} \delta_{jy}),$$

$$[A_1, \tilde{R}_{2j}] = \frac{i\sqrt{2}}{2} (S_{rx} \delta_{jx} - S_{ry} \delta_{jy}),$$

$$[A_2, \tilde{R}_{2j}] = -\frac{i\sqrt{2}}{2} (S_{ry} \delta_{jx} + S_{rx} \delta_{jy}),$$

$$[A_3, \tilde{R}_{2j}] = i (S_{lx} \delta_{jx} + S_{ly} \delta_{jy}),$$

$$[A_1, A_2] = -i (S_{lz} + S_{rz}), \quad [A_1, A_3] = [A_2, A_3] = 0,$$

Here j, k, m are Cartesian indices, $a = l, r$; $\mu, \nu = 1, 2$; $n = 1, 2, 3$; $\tau_{jkm}^{a\mu\nu}$, $\alpha_{jk}^{a\mu n}$, $\tilde{\alpha}_{jk}^n$ and β_{jkm}^μ are the structural constants, $\tau_{jkm}^{l\mu\nu} = \tau_{jkm}^{r\bar{\mu}\bar{\nu}}$, $\alpha_{jk}^{l\mu n} = -\alpha_{jk}^{r\bar{\mu} n}$ ($\bar{1} = 2$, $\bar{2} = 1$). Their non-zero components are:

$$\begin{aligned}
\tau_{xxz}^{l11} &= \tau_{xzx}^{l11} = \tau_{yyz}^{l11} = \tau_{yzy}^{l11} = \frac{1}{2}, \\
\tau_{xzx}^{l21} &= \tau_{yzy}^{l21} = \tau_{xxz}^{l12} = \tau_{yyz}^{l12} = -\frac{1}{2}, \\
\tau_{xyz}^{l11} &= \tau_{xyz}^{l12} = \tau_{yxx}^{l21} = \frac{i}{2}, \\
\tau_{xzy}^{l11} &= \tau_{yxx}^{l11} = \tau_{yxx}^{l12} = \tau_{xzy}^{l21} = -\frac{i}{2}, \\
\tau_{zzz}^{l11} &= 1, \quad \tau_{zzz}^{l22} = -1, \quad \tau_{zxy}^{l22} = i, \quad \tau_{zyx}^{l22} = -i, \\
\alpha_{xy}^{l11} &= \alpha_{yx}^{l11} = \frac{\sqrt{2}}{2}, \quad \alpha_{xy}^{l12} = \alpha_{yx}^{l12} = -\frac{\sqrt{2}}{2}, \\
\alpha_{xx}^{l11} &= \alpha_{xx}^{l12} = \frac{i\sqrt{2}}{2}, \quad \alpha_{yy}^{l11} = \alpha_{yy}^{l12} = -\frac{i\sqrt{2}}{2}, \\
\alpha_{xx}^{l23} &= \alpha_{yy}^{l23} = -i\sqrt{2}, \\
\beta_{xxz}^1 &= \beta_{yyz}^2 = -\frac{1}{2}, \quad \beta_{xxz}^2 = \beta_{yyz}^1 = \frac{1}{2}, \\
\beta_{xyz}^1 &= \beta_{xyz}^2 = \frac{i}{2}, \quad \beta_{yxx}^1 = \beta_{yxx}^2 = -\frac{i}{2}, \\
\beta_{xzy}^1 &= \beta_{zyx}^2 = -i, \quad \beta_{yxx}^1 = \beta_{zyx}^2 = i, \\
\tilde{\alpha}_{xx}^1 &= \tilde{\alpha}_{zz}^3 = i\sqrt{2}, \quad \tilde{\alpha}_{xy}^2 = \tilde{\alpha}_{yx}^2 = \tilde{\alpha}_{yy}^1 = -i\sqrt{2}.
\end{aligned}$$

The following relations hold,

$$\begin{aligned}
\mathbf{S}_a \cdot \mathbf{R}_l &= \mathbf{S}_a \cdot \tilde{\mathbf{R}}_3 = 0, \quad A_1 A_3 = A_2 A_3 = 0, \\
\mathbf{S}_a^2 &= 2X^{\mu_a \mu_a}, \quad \tilde{\mathbf{R}}_1 \cdot \tilde{\mathbf{R}}_1^\dagger + \tilde{\mathbf{R}}_2 \cdot \tilde{\mathbf{R}}_2^\dagger = 2X^{\mu_l \mu_l} + 2X^{\mu_r \mu_r}, \\
\mathbf{R}_l^2 &= X^{\mu_l \mu_l} + 3X^{S_l S_l}, \quad \tilde{\mathbf{R}}_3^2 = X^{\mu_r \mu_r} + 3X^{S_l S_l}, \\
A_1^2 + A_2^2 + A_3^2 &= X^{\mu_l \mu_l} + X^{\mu_r \mu_r}. \tag{C2}
\end{aligned}$$

Therefore, the vector operators \mathbf{S}_l , \mathbf{S}_r , \mathbf{R}_l , $\tilde{\mathbf{R}}_i$ and scalar operators A_i ($i = 1, 2, 3$) generate the algebra o_7 in a representation specified by the Casimir operator

$$\mathbf{S}_l^2 + \mathbf{S}_r^2 + \mathbf{R}_l^2 + \sum_{i=1}^2 \tilde{\mathbf{R}}_i \cdot \tilde{\mathbf{R}}_i^\dagger + \tilde{\mathbf{R}}_3^2 + \sum_{i=1}^3 A_i^2 = 6 \tag{C3}$$

APPENDIX D: YOUNG TABLEAUX CORRESPONDING TO VARIOUS SYMMETRIES

A TQD with "passive" central dot and "active" side dots reminds an artificial atom with inner core and external valence shell. The many-electron wave functions in this nanoobject may be symmetrized in various ways, so that each spin state of N electrons in the TQD is characterized by its own symmetrization scheme. One

may illustrate these schemes by means of the conventional graphic presentation of the permutation symmetry of multi-electron system by Young tableau³⁶. For instance, triplet state of two electrons which is symmetric with respect to the electron permutation is labeled by a row of two squares $\square\square$, whereas the singlet one which is antisymmetric with respect to the permutation is labeled by a column of two squares $\square|\square$. Having this in mind we can represent the singlet and triplet four electron states of the TQD (A5) by the four tableaux shown in Fig.10. The tableaux S_l (S_r) and T_l (T_r) correspond to the singlet and triplet states in which the right (left) dot contains two electrons (grey column in Fig.10) whereas electrons in the left (right) and central dots form singlet and triplet, respectively.

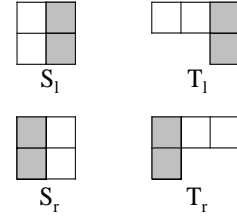


FIG. 10: Young tableaux corresponding to the singlet (S_a) and triplet (T_a) four electron states of the TQD. The grey column denote two electrons in the same dot (right or left).

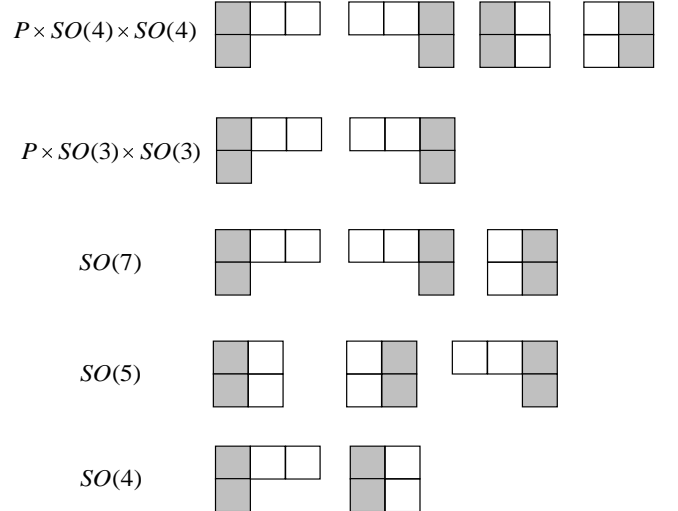


FIG. 11: Young tableaux corresponding to $SO(n)$ symmetries.

The Young tableaux corresponding to various $SO(n)$ symmetries discussed in Sec.III can be obtained combining the appropriate tableaux (Fig. 11). The highest possible symmetry $P \times SO(4) \times SO(4)$ is represented by four tableaux T_l , T_r , S_l and S_r since all singlet and triplet states are degenerate in this case. The symmetry $P \times SO(3) \times SO(3)$ occurs when two triplets T_l and T_r are close in energy and these are represented by the couple of

Young tableaux in the second line. Following this procedure, the $SO(7)$ symmetry can be described in terms of two triplets T_l , T_r diagrams and one singlet S_l diagram. Moreover, $SO(5)$ symmetry is represented by two singlet

S_l , S_r diagrams and one triplet T_l diagram and, finally, one triplet and one singlet tableaux correspond to the $SO(4)$ symmetry.

¹ *Atomic and Molecular Wires*, edited by C. Joachim and S. Roth (Kluwer, Dordrecht, 1996); L.P. Kouwenhoven, D.G. Austing and S. Tarucha, *Rep. Progr. Phys.* **64**, 701 (2001).

² *Nanophysics and Bio-Electronics*, edited by T. Chakraborty, F. Peeters, and U. Sivan (Elsevier, Amsterdam, 2002).

³ F. Guinea and G. Zimanyi, *Phys. Rev. B* **47**, 501 (1993); R. Mukhopadhyay, C.L. Kane, and T. C. Lubensky, *Phys. Rev. B* **63**, 081103 (2001); I. Kuzmenko, S. Gredeskul, K. Kikoin, and Y. Avishai, *Phys. Rev. B* **67**, 115331 (2003).

⁴ B.J. van Wees, H. van Houten, C.W.J. Beenakker, J.G. Williamson, L.P. Kouwenhoven, D. van der Marel, and C.T. Foxon, *Phys. Rev. Lett.* **60**, 848 (1988); K.J. Thomas, J.T. Nicholls, N.J. Appleyard, M.Y. Simmons, M. Pepper, D.R. Mace, W.R. Tribe, and D.A. Ritchie, *Phys. Rev. B* **58**, 4846 (1998).

⁵ S. Hershfield, J.H. Davies, and J.W. Wilkins, *Phys. Rev. Lett.* **67**, 3720 (1991); Y. Meir, N.S. Wingreen, and P.A. Lee, *Phys. Rev. Lett.* **70**, 2601 (1993); M.H. Hettler, J. Kroha, and S. Hershfield, *Phys. Rev. B* **58**, 5649 (1998).

⁶ M. Pustilnik, Y. Avishai, and K. Kikoin, *Phys. Rev. Lett.* **84**, 1756 (2000); M. Eto and Yu. Nazarov, *Phys. Rev. Lett.* **85**, 1306 (2000); D. Giuliano and F. Tagliacozzo, *Phys. Rev. B* **63**, 125318 (2001).

⁷ A. de-Shalit and I. Talmi, *Nuclear Shell Theory*, Academic Press, New York and London (1963).

⁸ Y. Goldin and Y. Avishai, *Phys. Rev. Lett.* **81**, 5394 (1998), *Phys. Rev. B* **61**, 16750 (2000); K. Kikoin, M. Pustilnik, and Y. Avishai, *Physica B* **259-261**, 217 (1999); K.A. Kikoin and Y. Avishai, *Phys. Rev. B* **62**, 4647 (2000); T.V. Shahbazyan, I.E. Perakis, and M.E. Raikh, *Phys. Rev. Lett.* **84**, 5896 (2000); T. Fujii and N. Kawakami, *Phys. Rev. B* **63**, 054414 (2001).

⁹ A. Yacobi, M. Heiblum, D. Mahalu, and H. Shtrikman, *Phys. Rev. Lett.* **74**, 4047 (1995); Y. Li, M. Heiblum, and H. Strikman, *Phys. Rev. Lett.* **88**, 076601 (2002); U. Gerland, J. von Delft, T.A. Costi, and Y. Oreg, *Phys. Rev. Lett.* **84**, 3710 (2000).

¹⁰ D. Goldhaber-Gordon, H. Shtrikman, D. Mahalu, D. Abush-Magder, U. Meirav, and M.A. Kastner, *Nature* **391**, 156 (1998); S.M. Cronenwett, T.H. Oosterkamp, and L.P. Kouwenhoven, *Science* **281**, 540 (1998).

¹¹ G.A. Fiete, J.S. Hersch, and E.J. Heller, *Phys. Rev. Lett.* **86**, 2392 (2001); M.A. Schneider, *Phys. Rev. B* **65**, 121406 (2002); J. Park, A.N. Pasupathy, J.I. Goldsmith, C. Chang, Y. Yaish, J.R. Petta, M. Rinkoski, J.P. Sethna, H.D. Abruna, P.L. McEuen, and D.C. Ralph, *Nature* **417**, 722 (2002); W. Liang, M.P. Shores, M. Bockrath, J.R. Long, and H. Park, *Nature* **417**, 725 (2002).

¹² L. Glazman and M. Raikh, *JETP Lett.* **47**, 452 (1988); T.-K. Ng and P. A. Lee, *Phys. Rev. Lett.*, **61**, 1768 (1988).

¹³ K. Kikoin and Y. Avishai, *Phys. Rev. Lett.* **86**, 2090 (2001).

¹⁴ K. Kikoin and Y. Avishai, *Phys. Rev. B* **65**, 115329 (2002).

¹⁵ T. Kuzmenko, K. Kikoin and Y. Avishai, *Phys. Rev. Lett.* **89**, 156602 (2002).

¹⁶ M.J. Englefield, *Group Theory and the Coulomb Problem* (Wiley, New York, 1972); I.A. Malkin and V.I. Man'ko, *Dynamical Symmetries and Coherent States of Quantum Systems* (Fizmatgiz, Moscow 1979).

¹⁷ J. Hubbard, *Proc. Roy. Soc. A* **285**, 542 (1965); see also Yu.P. Irkhin, *Sov. Phys. - JETP* **50**, 379 (1966).

¹⁸ The Coulomb potential possesses occasional degeneracy of the states with different moments \mathbf{l} . So, according to (3) the Runge-Lenz vector is the integral of motion. In this case one speaks about *hidden symmetry* of the system.

¹⁹ Y. Dothan, M. Gell-Mann and Y. Neeman, *Phys. Lett.* **17**, 148 (1965).

²⁰ P. W. Anderson, *J. Phys. C.: Solid. St. Phys.*, **3**, 2435 (1970).

²¹ F. D. M. Haldane *Phys. Rev. Lett.* **40**, 416 (1978).

²² M. Pustilnik and L.I. Glazman, *Phys. Rev. B* **64**, 045328 (2001).

²³ M. Eto and Yu. Nazarov, *Phys. Rev. B* **66**, 153319 (2002).

²⁴ R.N. Cahn, *Semi-Simple Lie Algebras and their representations* (Benjamin, 1984).

²⁵ J. Nygård, D.H. Cobden and P.E. Lindelof, *Nature* **408**, 342 (2000); N S. Sasaki, S. De Franceschi, J.M. Elzermann, *et al.*, *Nature*, **405**, 764 (2000).

²⁶ A.C. Hewson, *The Kondo problem to Heavy Fermions* (Cambridge University Press, 1997).

²⁷ B.A. Jones and C.M. Varma, *Phys. Rev. B* **40**, 324 (1989).

²⁸ A.M. Tsvelik and P.B. Wiegmann, *Adv. Phys.* **32**, 453 (1983).

²⁹ P.W. Anderson, G. Yuval and D.R. Hamann, *Phys. Rev. B* **1**, 4464 (1970); H. Shiba, *Progr. Theor. Phys.* **43**, 601 (1970).

³⁰ D.L. Cox and A. Zawadowski, *Adv. Phys.* **47**, 599 (1998).

³¹ I.S. Sandalov and A.N. Podmarkov, *Sov. Phys. JETP* **61**, 783 (1985).

³² One should also mention in this context the $SU(4) \supset SO(5)$ algebraic structure of superconducting and antiferromagnetic coherent states in cuprate High- T_c materials discussed by L-A. Wu, M. Guidry, Y. Sun and C-L. Wu, *Phys. Rev. B* **67**, 014515 (2003).

³³ J.R. Schrieffer and P.A. Wolff, *Phys. Rev.* **149**, 491 (1966).

³⁴ T. Kuzmenko, K. Kikoin and Y. Avishai, *cond-mat/0211281*.

³⁵ P. Nozieres and A. Blandin, *J. Phys. (Paris)* **41**, 193 (1980).

³⁶ J.P. Elliot and P.G. Dawber, *Symmetry in Physics* (Oxford University Press, 1984).